

# The distribution of dark and luminous matter inferred from extended rotation curves.

Roelof Bottema<sup>1</sup> and José Luis G. Pestaña<sup>2</sup>

<sup>1</sup>*Kapteyn Astronomical Institute, PO Box 800, NL-9700 AV Groningen, The Netherlands, robot@astro.rug.nl*

<sup>2</sup>*Departamento de Física, Universidad de Jaén, Campus Las Lagunillas, 23071 Jaén, Spain, jlg@ujaen.es*

Accepted: date1. Received: in original form:

## ABSTRACT

A better understanding of the formation of mass structures in the universe can be obtained by determining the amount and distribution of dark and luminous matter in spiral galaxies. To investigate such matters a sample of 12 galaxies, most with accurate distances, has been composed of which the luminosities are distributed regularly over a range spanning  $2\frac{1}{2}$  orders of magnitude. Of the observed high quality and extended rotation curves of these galaxies decompositions have been made, for four different schemes, each with two free parameters. For a “maximum disc fit” the rotation curves can be well matched, yet a large range of mass-to-light ratios for the individual galaxies is required. For the alternative gravitational theory of MOND the rotation curves can be explained if the fundamental parameter associated with MOND is allowed as a free parameter. Fixing that parameter leads to a disagreement between the predicted and observed rotation curves for a few galaxies. When cosmologically motivated NFW dark matter halos are assumed, the rotation curves for the least massive galaxies can, by no means, be reproduced; cores are definitively preferred over cusps. Finally, decompositions have been made for a pseudo isothermal halo combined with a universal M/L ratio. For the latter, the light of each galactic disc and bulge has been corrected for extinction and has been scaled by the effect of stellar population. This scheme can successfully explain the observed rotations and leads to sub maximum disc mass contributions. Properties of the resulting dark matter halos are described and a ratio between dark and baryonic mass of  $\sim 9$  for the least, and of  $\sim 5$ , for the most luminous galaxies has been determined, at the outermost measured rotation.

**Key words:** Galaxies: general – galaxies: halos – galaxies: kinematics and dynamics – galaxies: spiral – cosmology: dark matter.

## 1 INTRODUCTION

It is now a firmly established result that there is a large discrepancy between the visible, luminous mass in a galaxy and the dynamical mass. Observed rotation curves, especially those derived from the neutral hydrogen line, remain mainly flat in the outer regions. However, the light distribution, which generally decreases exponentially predicts that these rotation curves should be declining. This discrepancy can be explained by invoking dark matter (DM) surrounding the visible component as an extended more or less spherical mass component (Sancisi & van Albada 1987; Knapp & Kormendy 1987; Trimble 1987). The first detailed observations of extended H I rotation curves (Bosma 1978; Begeman 1987, 1989) were made of intermediate sized galaxies. These systems generally show a rotation which remains flat over a very large range of radii. Such a situation can only be generated if the rotational contribution of the inner luminous compo-

nent and that of the outer dark component conspire to make a combined curve at a constant level (the “conspiracy”, van Albada & Sancisi 1986). Later on it became evident that less luminous galaxies have rotations which continue to rise in the outer parts while the most luminous, and certainly the galaxies with a more concentrated light distribution, have a rotation which rises quickly near the centre and declines slightly in the outer regions. In that way the conspiracy does not exist any more (Casertano & van Gorkom 1991; Persic et al. 1996).

Naively one could reason that by subtracting the rotational contribution of the luminous component from the total observed rotation, the rotational signature of the dark halo remains. The principle is right, but in practice although the radial functionality of the luminous rotation can be derived quite accurately, the absolute contribution is difficult to quantify. The unknown luminous scale factor might be determined by making a least squares fit of the total com-

bined rotation to the observations. In most cases such a fit converges to a maximal contribution for the luminous mass, but a close inspection of the fit procedure shows that the solution is highly degenerate: nearly equally good fits can be achieved when exchanging dark for luminous matter (van Albada & Sancisi 1986; Dutton et al. 2005). Consequently, when doing such fits, constraints have to be set to either kind of matter. One of such constraints is the maximum disc hypothesis which states that the amount of luminous matter should be maximized. There are no principle reasons why this constraint should apply, but it has the useful feature that the procedure minimizes the amount of dark matter which is needed. Thus making the dark matter problem as small as possible. Furthermore it sets a firm upper limit to any determined mass-to-light (M/L) ratio of a galactic disc or bulge.

In principle the amount of mass in a disc (or bulge) can be determined by measuring the velocity dispersion of the stellar content. Such observations of stellar discs and the subsequent analyses are not straightforward and consequently reliable measurement have so far only been obtained for a few samples of galaxies. Yet such studies now generate a mounting evidence that a disc is sub maximal. From measurements of stellar velocity dispersions of a sample of inclined galaxies Bottema (1993) determined that, on average, the maximum contribution of a stellar disc to the total rotation is 63% with an error of some 10%. These observations and findings have been confirmed by Kregel et al. (2005) for edge-on disc galaxies, by Herrmann & Ciardullo (2009) by measuring the kinematics of planetary nebulae, and by Martinsson et al. (2013) for more face-on systems. The latter analysis even seems to indicate that the disc rotational contribution is smaller than the 63% mentioned above. There is additional evidence for such a sub maximum disc from a statistical analysis of rotation curve shapes in relation to the compactness of discs (Courteau & Rix 1999).

An alternative assessment of the matter of disc contribution can be made by considering mass-to-light ratios. The Initial Mass Function (IMF) seems to be universal for a range of normal galactic conditions (Kroupa 2001). That implies that identical stellar populations have identical mass-to-light ratios. By considering a broad spectrum of galaxy formation scenarios and a number of different population synthesis codes, Bell & de Jong (2001) establish a tight relation between the optical colour of a galaxy and its M/L ratio in every optical and near infra-red passband. This relation is well established, but the absolute value of the M/L ratio depends on the adopted IMF. If the low mass end of the IMF changes then also the M/L changes, typically for a standard Salpeter IMF (Salpeter 1955) with slope 1.35,  $M/L \propto m_l^{-0.35}$  where  $m_l$  is the low mass cutoff. Thus, one is back at square one: it is not possible to know the luminous mass contribution a priori. Anyhow, the relative functionality of Bell & de Jong is very useful because it allows a mass scaling of the observed population, like the preliminary procedure used by Bottema (1997). For instance, a red population is relatively old and deficient in light and so its associated mass should be scaled up. On the other hand, a blue population is young and bright and its light has to be scaled down to get the appropriate mass.

Historically, when dealing with the distribution of dark matter in the context of extended rotation curves, a ra-

dial density functionality is used equal to that of a pseudo isothermal sphere (Carignan & Freeman 1988, Begeman 1989). Objects of this sort are indeed produced by gravitational instabilities of a universal fluid having density fluctuations of a specified plausible form (Silk 1987). But recent detailed calculations and simulations of the formation of mass structures in the universe seem to require dark matter of a collisionless and cold kind. Such CDM (Cold Dark Matter) is able to explain, with considerable success, the observed filamentary and honey-comb structures of clusters and superclusters (Davis et al. 1985; Bond et al. 1996), appearing with the right sizes and at the right times. Collisionless matter entities get shaped by continued interactions, merging, and violent relaxation of smaller aggregates into larger structures. Inevitable that forms dark halos with density profiles close to that of an NFW (Navarro, Frenk, & White 1997) shape. Such a profile has an inner functionality proportional to  $R^{-1}$  (cusp) while a pseudo isothermal halo has a central core with constant density. In any way, it seems natural to assume that dark halos of present day galaxies should have a shape similar to that of an NFW profile.

Despite its success in explaining the large scale structures, CDM predicts a number of details which are not in agreement with observations. The three disagreements which stand out are: the expected cusps while cores are observed, the expected large number of dwarf satellites which should orbit a larger galaxy, which are not there, and the expected triaxiality of DM halos which is not observed. The first item of this list has been considered and discussed extensively in the recent literature. For example, there are a number of observations of the rotation in small or LSB galaxies, where the DM should dominate, which clearly show that the dark halos of these galaxies have cores (de Blok et al. 2001a,b, 2003; Salucci et al. 2003; Simon et al. 2003; Blais-Ouellette et al. 2004; Gentile et al. 2004). Several mechanisms have been invented to alleviate or modify the CDM predictions (see Peñarrubia et al. 2012, and references there in). One of the most promising seems to be cusp flattening by supernova explosions after an idea by Read & Gilmore (2005) and studied extensively by Governato et al. (2010) and by Pontzen & Governato (2012). Yet, in order to accomplish this, baryonic matter has to flow into the central regions of primeval galaxies until over there the density becomes comparable to that of the dark matter. Star formation has then to be suppressed until such densities are reached and subsequently an order of magnitude of the baryonic mass has to be expelled by SN explosions, taking along the central DM to the outer regions. It remains a matter of debate if this mechanism can actually work or whether it is in agreement with observed star formation histories and metallicity content of galaxies. For the smaller systems and certainly for dwarf spheroidals the energy requirements contradict such a scenario (Peñarrubia et al. 2012; Garrison-Kimmel et al. 2013).

As an alternative to dark matter the suggestion has been put forward that the usual law of Newtonian gravity breaks down on the scale of galaxies. In particular there is the proposal by Milgrom (1983) that the effective law of attraction becomes more like  $1/r$  in the limit of low accelerations. This proposal designated as MOND: Modified Newtonian Dynamics, has been successful in explaining certain aspects of the difference between luminous and dynam-

ical rotation on the scale of galaxies and groups of galaxies (Sanders 1990; Sanders & McGaugh 2002). MOND has been generalized and moulded into a relativistic theory with appropriate yet complicated field equations (Bekenstein 2004). If this theory proves to be comparable or superior to the DM paradigm it cannot be discarded as a toy model, and it could be the expression of a more fundamental principle.

Let's go back to the real world. MOND fitting has been applied to the rotation curves of galaxies in a number of studies. This fitting can and has been done in a few different ways depending on the number of allowed free parameters. In principle MOND is governed by one single acceleration parameter  $a_0$ , which has to be equal for all structures in the universe. For galaxies this leaves as a free parameter the amount of Newtonian contribution to the rotation, which can be parameterized by the M/L ratio of the luminous component. The contribution of the gas mass is fixed. Abandoning MOND as a fundamental theory, the acceleration parameter  $a_0$  can be considered as a free parameter too. This kind of fitting will be referred to as MOND-like and in first instance it can be used to check if indeed an equal value for  $a_0$  exists. In practice and certainly before accurately measured Cepheid distances became available, distance can be used as a third free fitting parameter, to within certain limits, of course. So in its broadest sense MOND fitting has three free parameters and as such can explain every available rotation curve with ease.

A first detailed analysis of the MOND method has been done by Begeman, Broeils & Sanders (1991, hereafter BBS). They selected a sample of only 10 galaxies with high quality and extended rotation curves. Most of these curves could be fitted with the MOND prescription using a universal value of  $a_0$  equal to  $1.21 \cdot 10^{-8} \text{ cm s}^{-2}$  with only slight adjustments to the Hubble distances. With one exception, being NGC 2841 which needed a MOND preferred distance twice as large as its Hubble distance. Well, one exception should confirm the rule. However, during the course of the Hubble key distance project a few Cepheid distances became available for galaxies in the sample of BBS. These distances are accurate to approximately 10% and appeared to differ in some cases considerably from the Hubble distances used before. Notably NGC 3198 was further away and NGC 2841 appeared to be closer than the preferred MOND distance. As analysed and discussed by Bottema et al. (2002, hereafter BPRS), it is really difficult to reconcile the distances of both these galaxies with a universal  $a_0$  parameter, unless one or more Cepheid distances are considerably wrong.

A few more studies have been done investigating the applicability of MOND in general and its consistency with observed rotation curves specifically. Different studies use different galaxy samples and a different number of free fitting parameters and are only generally comparable. For example de Blok & McGaugh (1998) consider a sample of 15 Low Surface Brightness (LSB) galaxies, which should reside largely in the weak acceleration or MOND regime and conclude that the MOND fit is excellent in 75% of the cases. Swaters et al. (2010) reach essentially the same conclusion for a larger sample of LSB galaxies. Gentile et al. (2011) consider 12 nearby galaxies for which rotation curves are available from the THINGS sample. For a MOND-like fit these authors find an average value for  $a_0$  essentially equal to the standard number of BBS. Fixing that value three quarters

of their sample can well be fitted; leaving distance as an additional free parameter all galaxies can be accommodated, as noted above. In a recent study of Randriamampandry & Carignan (2014) for a sample of 15 nearby galaxies, partly coinciding with the sample of Gentile et al, while keeping the  $(M/L)_{3.6\mu}$  ratio and the value of  $a_0$  fixed, find that only 60% of the galaxies can be made in agreement with the MOND prescription.

As part of a broader investigation of the distribution of dark matter in the present paper, also MOND has been considered. In first instance distances are now assumed to be known accurately. Then MOND-like fits are made to investigate how MOND with two free parameters compares with the procedure of adding DM with the same degree of freedom. In second instance it has been checked if the MOND philosophy works: can all rotation curves be explained with one universal  $a_0$  value for reasonable adjustments of the distances.

Presently the approach of BBS has been taken over: quality is preferred over quantity. A sample of 12 galaxies has been compiled of which 7 are in common with the sample of BBS. The requirement of a rotation curve extending beyond the edge of the optical disc is essential. If not, then certainly for the more massive galaxies, any fit to, or determination of the DM properties is usually possible, but meaningless. Four different schemes have been employed in decomposing the observed rotation curves. Each scheme uses a fitting method with two free parameters and are in that sense comparable. An extensive analysis is made of the quality and probability of each scheme; some work better, others are even ruled out. This all in an effort to find the most likely distribution of dark matter and to restrict the range of possible distributions.

This paper is organized as follows. In section 2 the sample is discussed and peculiarities of each galaxy have been specified. Section 3 gives a description of the extinction and population corrections in order to get a reliable amount of representative light for each system. In section 4 the rotation curve decomposition procedure is described in a general way. That procedure has been applied to the sample in section 5 for a maximum disc fit with pseudo isothermal halo. In section 6 MOND-like fitting and subsequent analysis of the MOND philosophy is presented. In order to relate the cosmologically motivated NFW halos to present day galaxies it is necessary to consider the process of adiabatic contraction. That process is described in section 7 and then incorporated into the fitting of NFW halos presented in section 8. In case of the more physically and observationally motivated scheme of an equal universal M/L ratio the fitting results are given in section 9, where also an extensive discussion is presented concerning the uncertainties and the Tully-Fisher relation (Tully & Fisher 1977). Finally in section 10 a more general discussion and point by point conclusions have been put together. Throughout, a Hubble constant of  $75 \text{ km s}^{-1} \text{ Mpc}^{-1}$  has been adopted.

## 2 THE SAMPLE OF GALAXIES

A sample of 12 galaxies has been composed based on the following criteria:

- (i) Rotation curves derived from a two dimensional radial velocity field.
- (ii) The velocity field should be regular and non-distorted, without large scale asymmetries.
- (iii) It should extend beyond the optical edge ( $\sim 5$  scale-lengths) of the disc.
- (iv) Inclinations larger than  $50^\circ$ , in order to derive, independently, the inclinations and rotation velocities from the velocity field.
- (v) Inclinations less than  $80^\circ$ , to avoid composite velocities along the line of sight.
- (vi) Photometry is available in a band redder (or equal to R.

and based on the following preferences:

- (i) Rotation curves extending as far as possible beyond the optical edge.
- (ii) A well determined distance, five galaxies have measured Cepheid distances.
- (iii) A velocity field and related rotation curve which are sampled by a sufficiently large number of independent data points.
- (iv) Optical emission line radial velocities in the inner regions when at those positions beam smearing of the H I data might be present.
- (v) Measured stellar velocity dispersions of the disc to have a handle on the local mass density.
- (vi) To generate a sample which is evenly spread over a large mass range.

Without any doubt there will be more than the 12 galaxies in the sample which satisfy the requirements, but we did not have the intention to be complete. The criteria and preferences above, can only be met when galaxies are observed in the neutral hydrogen line with an interferometer. A rotation curve is usually derived by a least squares fit to the velocity field of a collection of rings with radially variable inclinations, lines of nodes, and circular velocities. This procedure is described in detail by Begeman (1987, 1989). When H I data have been replaced by optical emission lines in the inner regions, the latter have on occasion been radially resampled to match the H I sampling. That ensures an equal radial weighting when doing the RC fit, which is a choice. Having more data points at a specific region may slightly change the relative contributions of the disc, bulge, and dark halo, but will not change any of the main results (see Blais-Ouellette et al. 1999).

The parameters and properties of the sample have been collected in the period 2003 to 2007 after which the analysis as presented in the remainder of this paper has been carried out. Because of personal reasons the work on this paper had to be abandoned for a while. During that time results of the THINGS (The H I Nearby Galaxy Survey; de Blok et al, 2008) had become available. Of the 12 galaxies in the present sample 6 are in common with the THINGS sample: NGCs 2403, 2841, 2903, 3198, 7331 and DDO 154. When comparing the H I rotation curves one can conclude that THINGS has a better radial sampling because observations have been done at a higher spatial resolution. But in general the observations do not have the signal-to-noise of the rotation curves already considered. The THINGS data then have a shorter radial extent for all the galaxies in com-

mon. Especially, in order to determine the DM distribution, these outer data points of the RC are of utmost importance and therefore, using the THINGS rotation curves instead of the present ones would not improve on the results.

The rotation curves appeared to be nearly identical at the positions where both are determined, except for DDO 154 where for the inner 3 kpc THINGS gives a larger rotation by a few  $\text{km s}^{-1}$  compared with the rotation curve of Carignan & Purton (1998) which had been used. Likely the latter suffers from beam smearing caused by the very limited spatial resolution. Therefore it appeared useful to take over the THINGS rotation curve for this specific case.

Over the past few years  $3.6\mu$  infrared photometry has become available for a number of galaxies from SINGS (Kennicutt et al. 2003), which has been used by de Blok et al. (2008) to characterize the luminous radial density distribution. When comparing these radial luminosity profiles with the ones of Kent (1986, 1987, hereafter K86 and K87) and Wevers et al (1986), in the Red bands one is struck by the similarity. This should not be obvious; radial absorption, population, and metallicity gradients might generate a difference between the red and infrared profiles. An explanation is left to others. Anyway, using the  $3.6\mu$  profiles instead of the present red profiles would not make a difference for the subsequent analysis or results. On the other hand, using the infrared luminosities would pose a serious problem for a population and a necessary metallicity correction for galaxies as a whole. Stellar population analyses in the infrared are exceptionally difficult and moreover the emission may be contaminated by a contribution of PAHs (polycyclic aromatic hydrocarbons). For photometry in the Red, population corrections are well described and the light is barely dependent on metallicity.

For all the galaxies a short description is now given of the adopted distances, photometry, and rotation curves. Uncertainties, peculiarities and references are quoted. In Table 1 a number of important parameter values are summarized.

## 2.1 NGC 2841

A distance of  $14.1 \pm 1.5$  Mpc has been determined by HST measurements of Cepheids (Macri et al. 2001). Photometry is available by K87 in the Thuan & Gunn (1976) r-band giving both, the photometric profile and total magnitude. Because there is a substantial difference in observed ellipticity between the bulge and disc a decomposition of the light of these components according to Kent's procedure is well determined. The H I rotation curve has initially been measured by Bosma (1981) and is later refined by Begeman (1987). The gas distribution is symmetric, but the kinematics displays a sizable amount of warping, making the determined rotation in the outer regions slightly less certain. The rotation curve remains more or less at a constant level all the way inwards to the centre. The THINGS rotation curve reaches out to 36 kpc and displays a sizable uncertainty between 25 and 36 kpc, while the present one goes out to 64 kpc, both are fully consistent.

## 2.2 NGC 3992

NGC 3992 is one of the most prominent members of the Ursa Major cluster of galaxies. Tully & Pierce (2000) determined a distance of 18.6 Mpc to this cluster, which will be adopted as the distance for NGC 3992. There is photometry in the BRIK' bands by Tully et al. (1996) of which the I profile is used to calculate the disc rotation and the R-band for the total light. The signature of the bulge is clearly present in the observed radial light profile and consequently the bulge to disc decomposition is straightforward. The H I rotation curve has been measured in detail by Bottema & Verheijen (2002), who also give a rotation curve decomposition. This galaxy has a bar and this bar region is devoid of gas so that no rotation is available for the inner regions.

## 2.3 NGC 7331

The HST Cepheid distance to this galaxy is  $14.72 \pm 0.60$  Mpc (Hughes et al. 1998; Freedman et al. 2001). Photometry is given by K87 in the r-band, but unfortunately the ellipticity of the central bulge and outer disc appear to be equal and Kent's decomposition procedure cannot be used. A detailed stellar and emission line kinematical study of the galaxy has been made by Bottema (1999). In that paper a decomposition into separate bulge and disc is presented, partly based on the observed stellar absorption line profiles. The bulge appears to be quite dominant and nearly spherical while the disc has an inclination consistent with the H I kinematical value of  $75^\circ$ . Unfortunately an error has turned up in Table 3 of Bottema (1999). For the favourite decomposition labelled "lpd" the total amount of disc and bulge light have been interchanged. The total light of disc and bulge should be  $11.4 \cdot 10^9 L_\odot^I$  and  $12.7 \cdot 10^9 L_\odot^I$  respectively and the b/d ratio is 1.1 instead of 0.9. The radial profile in the I band is given by Prada et al. (1996) which is used presently, although we have some doubt regarding the absolute calibration of this I-band photometry. Total R-band light is derived from K87. The H I rotation is determined by Begeman (1987), extending out to a radius of 37 kpc, and he supplements the rotation in the inner region with data of Rubin et al. (1965). However, as demonstrated by Bottema (1999) the gas kinematics in the inner regions of this galaxy is very unusual and certainly not representative for the gravitational potential. Therefore, at those positions the rotation as inferred from the stellar kinematics is adopted. The THINGS rotation curve only extends from a radius of 4 kpc to 24 kpc. The measured stellar velocity dispersion of the disc suggests that the contribution of the disc to the total rotation is small. This measurement is somewhat uncertain, however, because of the presence of a considerable amount of bulge light.

## 2.4 NGC 2998

NGC 2998 is the most distant galaxy of the sample. The radial velocity corrected for Virgo-centric flow gives a Hubble distance of 67.4 Mpc. Considering the deviations from the Hubble flow, this distance is nearly as accurate as the Cepheid distances for the galaxies more close by. Photometry is presented in K86; the galaxy is close to exponential

with only a minor bulge. For Kent's bulge-disc decomposition method the bulge has a luminosity of only 2% of that of the entire galaxy. Therefore, presently, the whole galaxy is considered as a disc structure, which effectively means that the mass-to-light ratio of the bulge is equal to that of the disc. An accurate H I rotation curve has been determined by Broeils (1992a), which has unfortunately not been published in the refereed literature. The velocity field is very symmetric and regular and the gas extends far beyond the optical edge. Because of its large distance the H I structure is not as well resolved as that of the more nearby galaxies and consequently the rotation curve is more sparsely sampled. Moreover, the observed kinematics in the inner regions is affected by beam smearing and cannot be used.

Absorption line spectroscopy is obtained along the whole major axis of NGC 2998, with a ( $1\sigma$ ) velocity resolution of  $25 \text{ km s}^{-1}$  (Bottema & Kregel 2014). From that, stellar radial velocities and stellar velocity dispersions have been derived extending to approximately two and a half optical scalelengths. In addition the emission lines of H $\beta$  and [O III] 5007 Å are observed, which have been combined to generate the rotation in the inner  $40''$ , there where the H I data are not useful. The emission line kinematics is symmetric, but slightly irregular, in the sense of showing some corrugation by less than  $10 \text{ km s}^{-1}$ . The stellar velocity dispersion decreases radially as expected for an exponential disc. Depending on the exact parameterization of the disc, a maximal contribution of the rotation of the stellar component to that of the total rotation is calculated. This value ranges between 0.64 and 0.72 with an error of 10%.

## 2.5 NGC 2903

The Hubble distance to this galaxy is 6.3 Mpc, while a distance estimate based on the brightest stars (Drozdovsky & Karachentsev 2000) is  $8.9 \pm 1.9$  Mpc. Presently we take as distance the average of the two: 7.6 Mpc. Photometry is measured by K87 giving the profile and total light. The rotation curve is composed of H $\alpha$  emission line data by Marcelin et al. (1983) for the inner  $100''$  and H I data by Begeman (1987) beyond, out to 29 kpc. The H $\alpha$  radial velocity measurements have been transformed into a rotation curve using the same inclination of  $62^\circ$  as for the H I kinematics. The THINGS rotation curve goes out to 25 kpc.

## 2.6 NGC 3198

The distance of  $13.8 \pm 0.5$  Mpc is derived from the HST Cepheid observations of this galaxy (Kelson et al. 1999; Freedman et al. 2001), and is considerably larger than the Hubble distance of 9.4 Mpc. Again, photometry by K87 is used of which the validity to represent the mass distribution is confirmed by K' band photometry by BPRS. Because the H I rotation curve (Begeman 1989) reaches very far out NGC 3198 has become the classic case of a spiral galaxy evidencing a large mass discrepancy in its outer regions (van Albada et al. 1985). Numerous re-observations of the H I and re-determinations of the rotation curve have been made. At the flat part none of these warrant a change to what had already been determined by Begeman (1989). Additionally all observations end at the radius of nearly 45 kpc probably because at larger galactocentric distances the H I gas becomes

ionized. The rotation curve of THINGS ends at a radius of 38 kpc. However that curve seems to show a somewhat lower rotation in the inner rising part, for  $R \lesssim 5$  kpc. Whether this is real or might be caused by a bar feature, needs to be confirmed. In this inner region of NGC 3198 matters appear to be quite complicated and a thorough analysis could easily fill a complete paper and is certainly beyond the scope of this study. Presently Begeman's curve has been taken over entirely with its relatively large errors in the inner region, nicely representing the current uncertainty.

For its size and mass NGC 3198 has indeed a relatively large amount of gas present (see Table 1). Stellar velocity dispersions of the disc of this galaxy have been measured by Bottema (1988), which for an assumed average disc thickness imply a sub maximum disc contribution to the rotation curve.

## 2.7 NGC 2403

This galaxy has a distance based on Cepheid variables (Freedman & Madore 1988; Freedman et al. 2001). Photometry by K87 and H I rotation curve by Begeman (1987). Like for NGC 3198 this galaxy has also been re-observed in the H I on numerous occasions, which has never led to any alteration of the rotation curve used here.

## 2.8 NGC 6503

A distance of  $5.2 \pm 1.1$  Mpc is assumed based on measurements of the luminosities of the brightest blue stars (Karachentsev & Sharina 1997), being in agreement with the Hubble distance of 4 Mpc and Tully-Fisher distance of 6 Mpc (Rubin et al. 1985). The luminosity profile is a composite of photographic Kodak IIIa-F measurements of Wevers et al. (1986) in the outer regions and R-band CCD photometry by Bottema (1989) in the inner regions. All is converted to R-band magnitudes. The H I rotation curve is from Begeman (1987). As for NGC 3198, stellar velocity dispersion observations (Bottema 1989) imply that the mass contribution of the disc is sub maximal.

## 2.9 NGC 5585

In this case the Hubble distance of 6.2 Mpc is the most reliable value available. Photometry in the B,V, and R-bands has been obtained by Côté et al. (1991) of which the R-band profile is used to calculate the rotation curve of the disc. This profile has been integrated to give the total R-band luminosity. An H I rotation curve is determined by Côté et al. from a regular though slightly warped velocity field. For radii within  $120''$  the rotation of Blais-Ouellette et al. (1999) based on H $\alpha$  Fabry-Perot observations is used. That inner rotation curve shows a specific bumpy feature which can be matched with the moderate central cusp in the photometry.

## 2.10 NGC 1560

The distance to this galaxy is taken as the average of three values. At first the Hubble distance of 3.25 Mpc. Secondly a distance of  $2.5 \pm 0.1$  Mpc (Lee & Madore 1993) based on bright stars and Tully-Fisher relation, and thirdly Krismer

et al. (1995) give a distance of  $3.5 \pm 0.7$  Mpc based on the TF relation. The average of the three amounts to 3.1 Mpc. Broeils (1992b) presents photometry in the B-band and Swaters & Balcells (2002) in the R-band. The profile of the latter authors declines slightly steeper and was used to represent the mass distribution of the disc. Total R-band luminosity also from Swaters. For radii beyond  $120''$  the H I rotation curve of Broeils (1992b) is adopted. Because this galaxy is rather edge-on ( $i \sim 80$  to  $82^\circ$ ) the available H I may be compromised by beam smearing and integration effects. Therefore long slit H $\alpha$  data of de Blok & Bosma (2002), which have kindly been made available by these authors) have been converted to rotational velocities. For such a high inclination galaxy slit data are not ideal. Yet this galaxy is large on the sky and one H $\alpha$  RC data point is the average of a lot of individual observations, showing quite some scatter, as expected. This average and associated error are judged to be sufficiently accurate. Between 120 and  $200''$  the H $\alpha$  and H I rotations are equal, for radii less than  $120''$ , the emission lines indicate a slightly larger rotation by approximately a few to  $10 \text{ km s}^{-1}$ . Therefore, at those positions the H $\alpha$  is used for the rotation.

## 2.11 NGC 3109

For this galaxy a Cepheid distance is available of  $1.36 \pm 0.10$  Mpc by Musella et al. (1997). These authors use the same distance to the LMC as the HST Cepheid distance key project and is in that sense comparable. Yet there may be small systematic differences between the two methods. Recently, Soszyński et al. (2006) determined a distance of  $1.30 \pm 0.04$  Mpc by extending the Cepheid observations to the infra-red. This confirms the value of Musella et al. and the difference is so small that we maintained the value of 1.36 Mpc. Uncalibrated I-band photometry has been obtained by Jobin & Carignan (1990) of which the radial profile was used to calculate the rotation of the disc. A total R-band luminosity was derived from the ESO LV catalogue (Lauberts & Valentijn 1989) by extrapolating the R-band aperture value at  $R_{26}$  equal to the B-band functionality.

The construction of the rotation curve is somewhat complicated. From the I-band photometry, assuming  $q_0 = 0.11$  one has an inclination of  $75^\circ$ , which seems well determined. H I observations of Jobin & Carignan suggest an inclination of  $70^\circ$  but is rather uncertain. Therefore the errors on the H I rotation have been increased to include this uncertainty in the inclination. For the inner regions ( $< 350''$ ) the rotational data have been supplemented with H $\alpha$  Fabry-Perot observations by Blais-Ouellette et al. (2001). In that paper an inclination is used of  $88^\circ$ , which is clearly in contradiction with other determinations. Therefore the rotation of Blais-Ouellette et al. has been converted to an inclination  $75^\circ$ . Moreover, the quoted errors appeared to be unrealistically small and have for all H $\alpha$  rotational data points been increased to  $5 \text{ km s}^{-1}$ . That should then also include any uncertainties associated with the asymmetric drift correction. This might all seem a bit tricky, but for a galaxy with such a large inclination small changes in the inclination never substantially affect the rotation.

## 2.12 DDO 154

A description of distances, photometry, and rotation can be found in the paper of Carignan & Beaulieu (1989). The distance of 3.8 Mpc is based on a combination of brightest star considerations and association with the Canes Venaticorum I cloud. Photometry is available in the B,V, and R bands. An additional measurement in the R-band by Swaters & Balcells (2002) is consistent, both concerning the profile and total luminosity.

The H I rotation curve of Carignan & Beaulieu exhibits a decline beyond a radius of  $\sim 300''$ . In a following study by Carignan & Purton (1998, hereafter CP98) additional observations reveal a more extended low level H I structure. The outer H I distribution is lopsided but the velocity field appears rather regular. Again the derived rotation curve starts to decline abruptly and continues so out to a radius beyond  $540''$ . The derivation of the rotation curve by these authors seems solid. As mentioned above, the rotation curve of THINGS qualifies to replace the one of CP98 because their inner data points have probably been affected by beam smearing. Moreover the errors which have been given are unrealistically small.

Then we encountered a problem. In the paper of De Blok et al. (2008) two different rotation curves for DDO 154 are presented, one slightly rising in the outer parts in their figures 15 and 46, and one nearly constant or decreasing slightly in their figure 81. The different rotation curves have been derived for a differently adopted inclination functionality between  $300''$  and  $400''$ , both of which are consistent with the THINGS observations. For this galaxy at those positions the tilted rings used to fit the velocity field are only partially and irregularly filled with data on hence an independent inclination determination is not possible. The observations of CP98 extend further out, until a radius of approximately  $540''$ ; their velocity field appears to be regular over there with an inclination nearly constant at  $60^\circ$ , which coincides with the choice of De Blok et al. in their figure 81. Consequently that rotation curve of THINGS is to be preferred and as such is completely compatible with the rotation curve of CP98. In this study that rotation curve has been taken over, supplemented with the data points at  $450''$  and  $540''$  of CP98 with an error increased to a realistic value of  $5 \text{ km s}^{-1}$  for an adopted inclination uncertainty of  $10^\circ$ .

The radial distribution of the gas has been taken from Carignan & Beaulieu (1989) for the inner regions. It has been extended to larger radii by a smooth matching to it with the distribution given in Fig. 4 of CP98.

## 3 TOTAL LIGHT IN R, EXTINCTION AND POPULATION CORRECTIONS

To obtain an amount of light which is representative for the amount of luminous matter in a galaxy corrections have to be made to the observed total light, in this case in the Kron-Cousins R-band. There are two main corrections to be made; a correction for absorption to be called extinction correction, and a correction for population. The latter is needed because a younger population generates more light compared to an older population for the same amount of

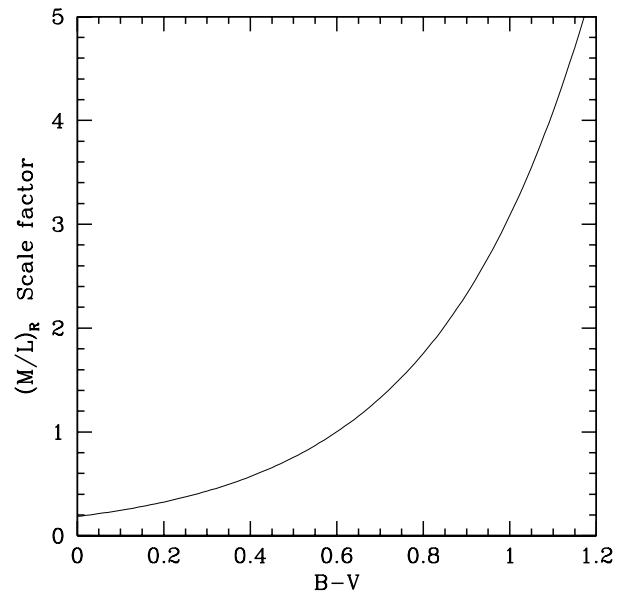


**Figure 1.** Mass-to-light ratio in the R-band as a function of B-V colour (Bell & de Jong 2001), lowered by 15.5% to give a value of 1.0 at B-V = 0.6. This relation is used to scale the amount of light in a galaxy to a representative value for the amount of mass.

stellar mass. Uncorrected parameters have been given the subscript “obs”, those corrected only for extinction “ec” and those corrected for extinction plus population are given the subscript “epc”.

### 3.1 Galactic extinction

Extinction from the local Galaxy, designated by  $A^b$  is taken from Schlegel et al. (1998). Its values for the sample of galaxies can be found, with other forthcoming corrections, in Table 2.

### 3.2 Internal extinction to face-on

A correction for this extinction ( $A^{i-0}$ ) is given by Tully et al. (1998) and depends on the absolute luminosity of a galaxy corrected for Galactic and internal extinction ( $M_R^{b,i-0}$ ) and on the observed aspect ratio  $a/b$  as

$$A_R^{i-0} = \gamma_R \log \left( \frac{a}{b} \right), \quad (1)$$

with

$$\begin{aligned} \gamma_R &= -0.24 (16.06 + M_R^{b,i-0}) \\ &= 0 \text{ if } M_R^{b,i-0} > -16.06. \end{aligned} \quad (2)$$

This correction has been applied separately to the disc and the bulge (see Table 2).

### 3.3 Intrinsic extinction of a face-on galaxy

This matter is uncertain because it has never been investigated in a systematic way. Therefore we can only give a reasonable estimate. Tully & Fouqué (1985) and Verheijen (2001) use an amount of intrinsic extinction ( $A_R^{i-0}$ ) of 0.21 mag. for an average galaxy in their samples. Comparing

these samples with the galaxies in this paper such an average galaxy has approximately the luminosity of NGC 3198. It is further assumed that the intrinsic extinction is smaller for less luminous galaxies, analogous to the extinction correction to face-on. Adopting  $A^{i=0} = \text{zero}$  for  $M_R^{b,i=0} > -16.0$  we use for  $M_R^{b,i=0} < -16.0$ :

$$A_R^{i=0} = -0.042 M_R^{b,i=0} - 0.672, \quad (3)$$

for discs and  $A_R^{i=0} = 0$  for bulges.

### 3.4 Population correction

Bell & de Jong (2001) calculate mass-to-light ratios for galaxies as a function of their colours. The existence of such a colour versus M/L ratio relation can be understood because a younger, lower M/L ratio population is relatively bluer compared to an older, larger M/L ratio population. Bell & de Jong demonstrate that such a relation is largely independent of galaxy evolution scenarios and on the employed population synthesis code. In the non near infra-red passbands it barely depends on metallicity of the population. For the M/L ratio in the R-band and B-V colour Bell & de Jong give a relation of

$$^{10}\log(M/L_R) = -0.66 + 1.222(B - V) \quad (4)$$

As for all population synthesis analyses the M/L ratio is only known up to a certain factor. This factor depends on the assumed low mass end of the IMF and might be as large as two. We can therefore not use Eq. (4) to derive M/L ratios, but we shall use it to correct the amount of R-band light for the excess amount of light of a young population, or deficiency of light of an old population. A fiducial B-V of 0.6 is chosen for which such a population correction is zero. Then, using Eq. (4) with M/L lowered by 15.5%, in Fig. 1 the scale factor is given with which the amount of light has to be multiplied to obtain the representative amount of mass.

In section 9 a successful fit to all rotation curves can be achieved by using an equal mass-to-light ratio in R, corrected for extinction and population, having a value of 1.0. This means that the scale factor presented in Fig. 1 is then exactly equal to the  $(M/L)_R$  ratio as a function of B-V colour one needs for galaxies in general. As a consequence the relation as calculated by Bell & de Jong, on the basis of hitting the default lower mass cutoff in the population synthesis codes of  $0.1 M_\odot$  is then 15.5% too large. If, instead, a lower mass cutoff at  $0.15 M_\odot$  would have been taken, their relation would be spot on the relation given in Fig. 1, and thus on what the successful rotation fit scheme of section 9 implies.

B-V colours of galaxies can be found in the RC3 (de Vaucouleurs et al. 1991), but in order to be usable in Eq. (4) should be corrected for absorption. For that we used the recipe given in the RC3, to obtain the parameter designated as  $(B - V)_T^0$ . Since rotation curve decompositions will be made with a separate disc and bulge, it appeared necessary to apply the extinction and population corrections separately to these components too. Unfortunately the  $(B - V)_T^0$  values are not listed separately, but can be retrieved. When the total observed  $(B - V)_{\text{obs}}$  is given (RC3), the ratio of disc to bulge light has been determined (Table 1), and the observed  $(B - V)_{\text{obs}}$  of the bulge is known, the observed

$(B - V)_{\text{obs}}$  of the disc can be derived. The B-V of the bulge has been assumed to be equal to the B-V colours of the smallest apertures given by Longo & de Vaucouleurs (1983). Subsequently the separate  $(B - V)_{\text{obs}}$  colours have been converted to  $(B - V)_T^0$  according to the RC3. The results of the population correction procedure are given in Table 3 for the sample of galaxies. Note that the three bulges are relatively red, the population is therefore old and light has to be scaled up considerably.

For all the forthcoming fits two kind of mass-to-light ratios will be presented; as observed,  $(M/L)_{\text{obs}}$  meaning with no correction at all and  $(M/L)_{\text{epc}}$  with both, the extinction and population correction applied. In Sect. 9 a decomposition is presented using an equal  $(M/L)_{\text{epc}}$  for all luminous galaxy components.

## 4 ROTATION CURVE FITTING

For every galaxy a model rotation curve is computed as the squared sum of the individual contributions of the disc, bulge, gas, and dark halo. The contribution of the gas is fixed by observations of the neutral hydrogen gas, of which the amount has been multiplied by a factor 1.4 to account for the presence of Helium and a small amount of ionized hydrogen. The disc and bulge light distribution are measured by the photometry of the galaxy. Scaling by the M/L ratio then gives the mass contribution. For the dark halo generally an analytical density functionality is assumed described by one or two parameters. Thus the composite model rotation curve has as free parameters the M/L ratio of the luminous components and the descriptives of the dark halo. This composite curve is then fitted in a least squares sense to the observed rotation curve, a procedure often referred to as decomposition of the rotation curve.

In that way the best fit is designated as the situation of a minimum  $\chi^2$  value. This procedure is scientific in the sense that it is reproduceable and therefore is preferred over, for example, an estimated fit by eye. Yet one has to be careful when applying this method. A least squares fitting procedure assumes that the fitting function is known a priori and that the data points scatter in a Gaussian way around that function. For rotation curves that is not valid. Firstly a rotational functionality for the halo is adopted which need not be correct. Secondly the procedure to determine the rotation is an approximation in the sense that azimuthal symmetry is assumed with no in or outflow. For example spiral arms can produce small irregularities, which may lead to small systematic deviations from the actual rotation law. In addition one has to be careful when "feeding" the fitting procedure. At positions with a high degree of sampling the fit is forced to a higher weight. Therefore, presently, rotation curves have, on occasion, been resampled to a nearly uniform radial distribution to give equal weight over the entire radial extent. Because of these matters the resulting minimum  $\chi^2$  value is only a limited indicator of the quality of the fit and it cannot be concluded from that value only that a certain dark halo functionality is better or worse.

The radial luminosity profiles of bulge and disc are adopted to indicate the radial mass distribution. This assumes that the M/L ratio is constant in the galaxy which can be justified by the observed small radial colour gradi-

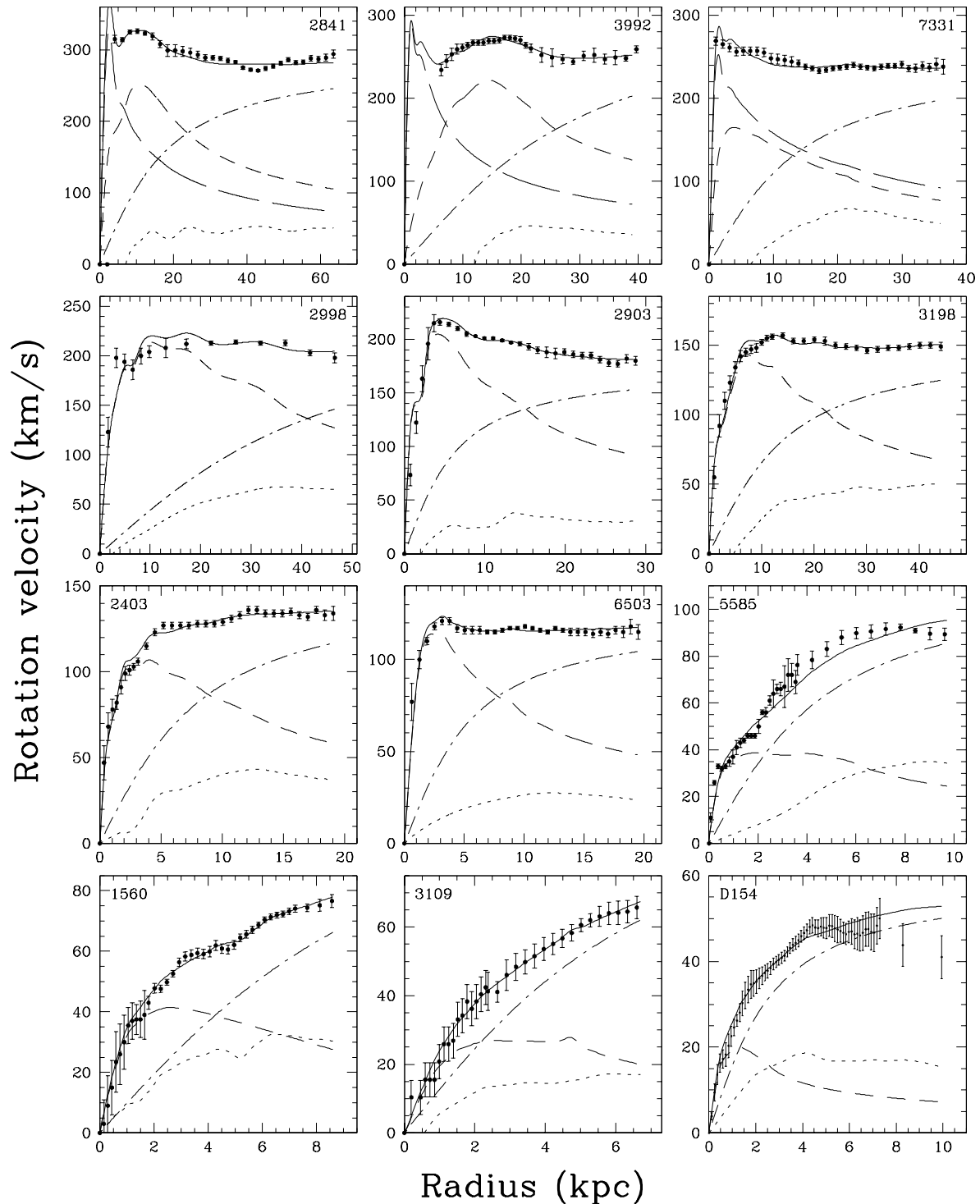


**Figure 2.** Maximum disc fits to the observed rotation curves (dots) of the 12 galaxies in the sample. Here, and in forthcoming similar plots (Figs 4, 7, and 9), the lines are coded as follows: full drawn is the fit, dotted, short-dashed, long-dashed and dash-dot lines represent the rotation of the gas, the disc, the bulge, and the pseudo isothermal dark halo, respectively. The observations can be matched quite accurately, except for NGC 5585 and DDO 154 which show a small discrepancy.

ents, in general (de Jong 1996), at least for normal quiescent systems. Nevertheless, in order to minimize dust and population effects and so to be close to the real mass distribution, a profile in a passband as red as possible is preferred. Currently for all galaxies of the sample the profile is in a (R)ed or near (I)nfared passband (see Table 1).

For the discs the observed radial mass distribution is combined with an adopted  $\text{sech}^2(z/z_0)$  vertical mass distribution with  $z_0$  being 0.2 times the value of the radial scalelength (van der Kruit & Searle 1981, 1982). The disc rotation curve is then calculated following Casertano (1983). For the bulge which is assumed to have a spherical distribution the rotational velocity can be calculated using the equations on page 1310 of K86. Both for the disc and the bulge the rotation curves can then be scaled up with the unknown M/L ratio. For the gas the radial mass distribution is observed directly. To calculate the rotation a thin vertical distribution is assumed. Finally the dark halo. In this paper a few density functionalities have been investigated usually parameterized by two values. A detailed description will be given where appropriate. The calculation of the rotations curves and the fitting procedures have been performed using the routines ROTMOD and ROTMAS in the GIPSY package.

In practice it appears that the fitting procedure is degenerate; one generally cannot determine the M/L ratio and dark halo parameters simultaneously. Consequently it is necessary to impose certain constraints. In the remainder of this paper, in principle, constraints are made such that there are always two free parameters left (or three with a bulge); in that sense the fitting schemes are then comparable.

## 5 MAXIMUM DISC AND BULGE FITS

In general the maximum disc constraint is associated with a dark halo functionality of a pseudo isothermal sphere (Carignan & Freeman 1988). For consistency that functionality will also be used presently. Its density distribution  $\rho_h$  takes the form

$$\rho_h = \rho_0 \left[ 1 + \frac{R^2}{R_{\text{core}}^2} \right]^{-1}, \quad (5)$$

with an associated rotation  $v_{\text{p.iso}}$  of

$$v_{\text{p.iso}} = v_{\text{max}}^h \sqrt{1 - \frac{R_{\text{core}}}{R} \arctan\left(\frac{R}{R_{\text{core}}}\right)}, \quad (6)$$

where the halo rotation becomes asymptotically flat at a maximum value of  $v_{\text{max}}^h$  which is related to the central density  $\rho_0$  and core radius  $R_{\text{core}}$  as

$$v_{\text{max}}^h = \sqrt{4\pi G \rho_0 R_{\text{core}}^2}. \quad (7)$$

Note that for small radii  $\rho_h \approx \text{constant}$  and  $v_{\text{p.iso}} \propto R$ , while for radii much larger than the core radius  $\rho_h \propto R^{-2}$  and  $v_{\text{p.iso}} \approx \text{constant}$ . Two free parameters describe the halo:  $R_{\text{core}}$  and  $v_{\text{max}}^h$ .

As mentioned in the previous section, a maximum disc fit assumes a maximum contribution to the rotation curve by the luminous components. For a system with only a disc this means in practice that one scales up the disc rotation in the inner regions as much as possible to be still consistent with the observations. In cases where there is a bulge too, because of its strong mass concentration, the bulge contribution has

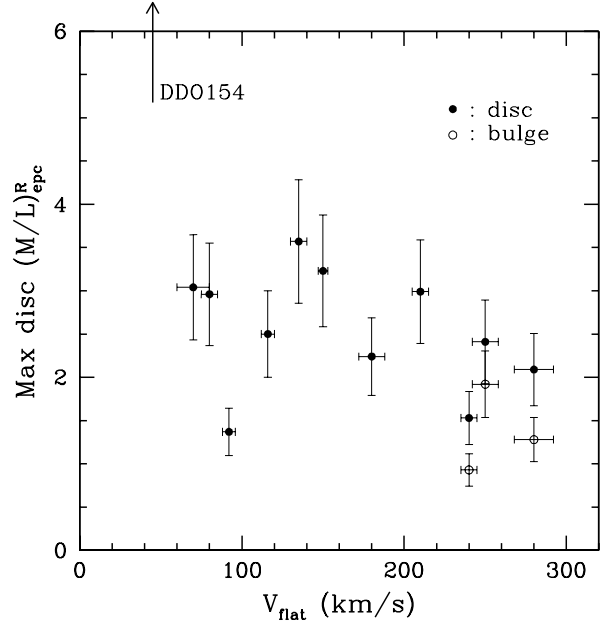


**Figure 3.** The M/L ratios, corrected for absorption and population effects, following from the maximum disc fits. Different galaxies are represented along the x-axis by their observed rotation at the flat, outer part of the rotation curve. There appears to be a trend in the sense that the more massive galaxies have a smaller M/L ratio.

to be maximized first followed by the disc. For systems with a bulge the rotation generally remains flat, going inwards to small radii. That implies that if the bulge were not maximal, a dark halo with very short core radius would be required. The maximum disc/bulge adjustment procedure can generally be done with approximately a 5% error in the bulge and disc rotation, which generates a 10% error in the M/L ratios.

For the 12 galaxies maximum disc fits are presented in Fig. 2. In most cases the fits to the observations are excellent; even certain small scale features in the photometry which are expressed in the model rotation curve appear to be reflected in the observations. Nevertheless for two cases, NGC 5585 and DDO 154, there is a small discrepancy at the outermost radii. It seems that the observed rotation drops while the model curves predict a continued rise. Whether we are witnessing a steep end to the dark halo for these two galaxies, or whether the observed drop is an artifact remains to be investigated further. In Table 4 the fitting parameters are presented. Errors of the mass-to-light ratios are estimated at 20%. That is a combination of the errors of the amount of light, caused by the various uncertainties of distance, extinction, and colour corrections effects, and the error generated by the fitting method (Sect. 10.3). The determined core radius is generally comparable in size to the radius of the last measured rotation point. That is a direct consequence of the maximization procedure of the disc which leads to a minimal amount of dark halo matter in the inner regions.

The determined M/L ratios corrected for absorption and population effects are given as a function of the observed rotation at the flat, outer part of the rotation curve

in Fig. 3. It can be noticed that the corrected M/L ratios of the discs have a range of at least a factor of two and a half. Minimum to maximum go from approximately 1.4 to 4 and to 9.2 for DDO154. There appears to be a trend in the sense that the more massive galaxies have a smaller corrected M/L ratio. Such an appreciable range has to be explained by different initial mass functions for the galaxies, while evidence so far suggest that the IMF is more or less universal for normal galaxies. One has to keep in mind, however, that the maximum disc hypothesis is just a hypothesis. In a more practical sense one can consider the determined M/L ratios as an upper limit. The smallest M/L ratio could then be the M/L ratio which applies for all galaxies. In this respect it is interesting to note that the  $(M/L)_{\text{epc}}$  ratios of the bulges are situated at the lower range of the values. An equal M/L ratio for all discs and bulges for all galaxies given by, for example, the smallest maximum disc M/L ratio would then imply that bulges remain close to the maximum contribution to the rotation in the inner regions. A comprehensive analysis of these matters is made in Sect. 9.

In Table 4 mass-to-light ratios are also given as observed, so with no corrections. As can be noticed, then there is a large, unrealistic, range of values. Consequently it is imperative that absorption and population corrections are made.

## 6 MOND FITS

### 6.1 Basics

As an alternative to dark matter, the flatness of rotation curves may be explained by a different law of gravity which prevails in the outer regions of galaxies. A rather successful such proposal is Milgrom's (1983) modified Newtonian dynamics or MOND. Here the idea is that below a certain acceleration threshold ( $a_0$ ) the effective gravitational acceleration approaches  $\sqrt{a_0 g_N}$  where  $g_N$  is the usual Newtonian acceleration. This modification yields asymptotically flat rotation curves of spiral galaxies and a luminosity – rotation velocity relationship of the observed form,  $L \propto v^4$ , the Tully-Fisher relation. MOND is able to explain in considerable detail the actual rotation curves of galaxies (BBS, Sanders 1996, Sanders & Verheijen 1998, McGaugh & de Blok 1998). In principle  $a_0$  should have one universal value and should not be allowed as a free parameter. In that sense MOND rotation curves are predictions and not fits (Milgrom 1988).

### 6.2 Two parameter MOND-like fits

In first instance, however, MOND will be considered here as a fitting procedure with  $a_0$  and M/L as two free parameters, and not as a phenomenological alternative to Newtonian gravity. As mentioned in the introduction, it is then compatible with the other three fitting procedures employed in this paper, who also use two free parameters. For the remainder, the two parameter MOND fit will be referred to as MOND-like fit, to avoid any confusion. To make this fit, in practice, a least squares fit to the observed rotation curve is made by having an acceleration  $g_{\text{mond}}$  equal to

$$g_{\text{mond}} = \frac{g_N}{\sqrt{2}} \left[ 1 + \sqrt{1 + 4 \left( \frac{a_0}{g_N} \right)^2} \right]^{1/2}, \quad (8)$$

where the Newtonian acceleration  $g_N$  is calculated from the mass distribution in the standard way. The circular velocity is then given as usual by  $v_{\text{rot}} = \sqrt{R g_{\text{mond}}}$ .

In Fig. 4 the MOND-like fits for the sample of galaxies are presented while fit parameters are listed in Table 5. No large discrepancies can be detected between the data and model rotation curves. For most galaxies and certainly for the more massive, the fits are impressive. But for three cases there are small yet noticeable deviations. For NGC 5585 the MOND-like fit gives too low rotations at intermediate radii. A better representation can certainly be achieved by using dark matter for a maximum disc situation (Sect. 5, Fig. 2), and especially for a slightly sub maximum disc case (Sect. 9, Fig. 9). Thus the blame for this misfit cannot be put straightforwardly on an incorrectly determined rotation curve. NGC 3109 has in the inner regions rotations which are slightly but systematically below the fit, but considering the errors this is not a real problem. More problematic is the obvious misfit in the outer regions of DDO 154. For the other three fitting procedures who use specified dark halo radial density laws there is the same misfit. Yet an explanation for the decreasing rotation curve can then always be found by a sudden end to the dark matter distribution. In case of MOND that is not possible: there is no dark matter and consequently the discrepant fit then poses a more serious problem.

For the larger galaxies MOND-like requires the discs to be maximal. This results in M/L ratios (Table 5) which are close to the values found when using the maximum disc constraint. Consequently also for MOND-like there appears to be a considerable range of M/L ratios, both for the absorption and population corrected and for the uncorrected M/L values. As to the likeliness of this one is referred to the discussions in the previous section.

### 6.3 The value of $a_0$

Figure 5 displays the fitted value of  $a_0$  versus the rotation of the galaxy at the flat, outer part of the rotation curve. There is a considerable scatter, which remains if only the galaxies with well determined Cepheid distances are considered. If the extreme upper and lower points are ignored there might even be a trend such that the more massive galaxies have a larger value of  $a_0$  as was already tentatively reported by Lake (1989). A comparison can be made with the values determined by Randriamampandy & Carignan (2014) for a fixed  $(M/L)_{3.6\mu}$  value. There appears to be a comparable distribution of  $a_0$  values; the scatter is comparable and there seems to be the same slight trend with galaxy mass. It thus appears that the MOND-like fitting procedure also needs two free parameters. As such it can then give a good description of the observed rotations of almost all of the galaxies in the sample. The fact that it is possible to reproduce the observed rotation curves without invoking dark matter inevitably points to a fundamental relation between the baryonic matter distribution and the observed large scale kinematics, whatever that might mean.

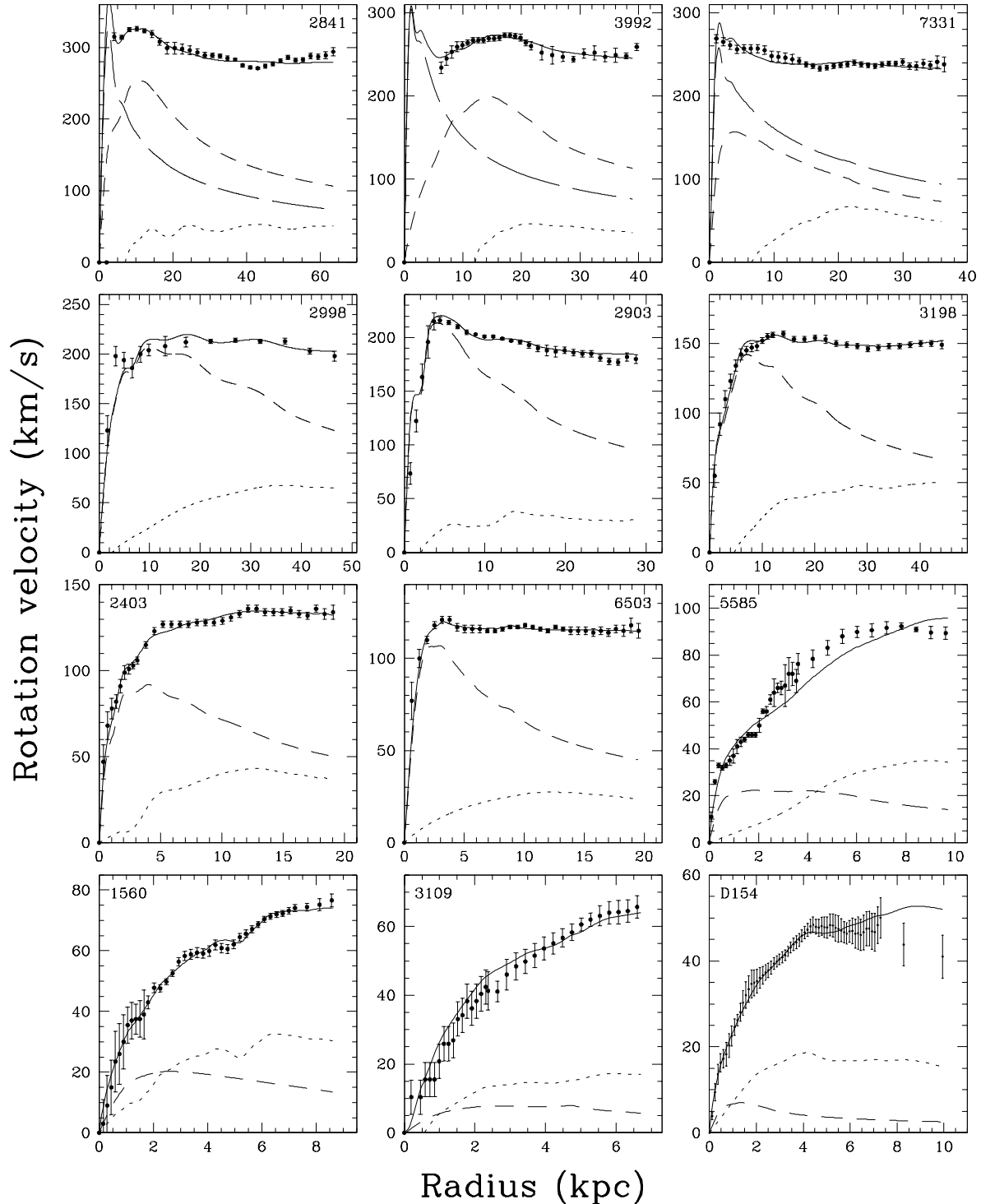


**Figure 4.** MOND-like fits to the observed rotation curves. Here MOND-like means that there are two free parameters: the  $M/L$  ratio of the disc (and bulge, if present) and the MOND scale  $a_0$ . For most galaxies the quality of the fit is excellent and comparable to that of the maximum disc case. However, for three galaxies, NGC 5585, NGC 3109, and DDO 154 the fits slightly deviate from the data.

From the perspective of Mondian philosophy, where one universal value of  $a_0$  is required, the data in Fig. 5 are not encouraging. For the same analysis made by BBS,  $a_0$  values are distributed more closely around a constant, with one exception for NGC 2841, and there is not a trend with mass

of the galaxy. At that time the distances to the objects were less accurate and moderate adjustments to the individual distances made it plausible that the rotation curves could be explained by MOND with a universal  $a_0$  value determined at

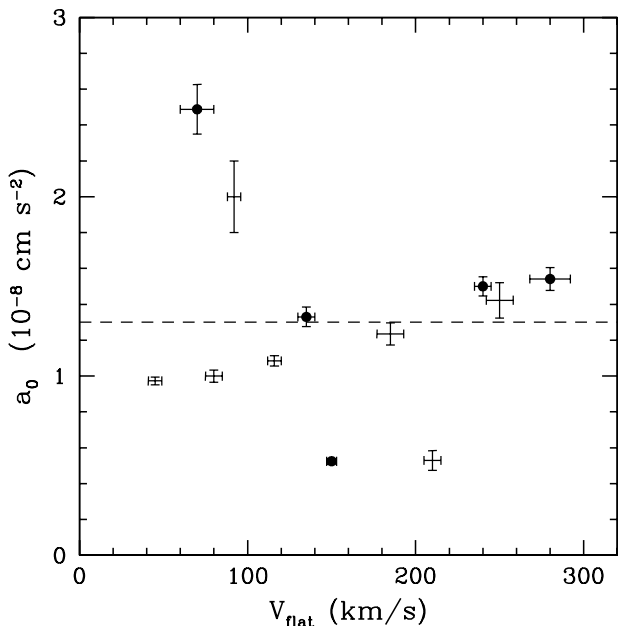


**Figure 5.** The value of the  $a_0$  parameter following from the MOND-like fits to the rotation curves of the sample. The data appear to be uncorrelated and to have a considerable scatter. Galaxies with Cepheid distances have been indicated by a dotted point, the dashed line is at the median value.

$1.21 \cdot 10^{-8} \text{ cm s}^{-2}$  by BBS. Since then this number has been generally used by various authors in a number of studies.

In reality, however, there appears to be a reasonable uncertainty concerning the universal value. Sanders & Verheijen (1998) give MOND fits to the rotation curves of 30 spiral galaxies in the UMA cluster which they assume to be at 15.5 Mpc. The preferred value of  $a_0$  with this adopted distance is equal to the BBS value. But, after a Cepheid based re-calibration of the T-F relation, Tully & Pierce (2000) argue that the distance to the UMA cluster should be taken at 18.6 Mpc. As discussed by BPRS the preferred value for  $a_0$  then has to be decreased to  $0.9 \cdot 10^{-8} \text{ cm s}^{-2}$ . That is also the preferred value of  $a_0$  from MOND fits to rotation curves of a sample of nearby dwarf galaxies with distances taken primarily from group membership (Swaters et al. 2010). Gentile et al. (2011) find an average essentially equal to the original BBS value, but Randriamampandry & Carignan determine an average  $a_0$  of  $1.13 \pm 0.50 \cdot 10^{-8} \text{ cm s}^{-2}$ . So, considering MOND as a real alternative to dark matter, what universal value should one adopt?

In the present analysis of which the sample largely overlaps that of BBS, there is clearly no indication that  $a_0$  should be decreased to  $0.9 \cdot 10^{-8} \text{ cm s}^{-2}$ . If one bears in mind the slight trend of a decreasing  $a_0$  for lower masses for eight galaxies, as noted above, it might be plausible that certainly the dwarf galaxies of Swaters et al. (2010) lead to a lower determination of  $a_0$ . Anyway, in first instance we take  $a_0$  to be equal to  $1.3 \cdot 10^{-8} \text{ cm s}^{-2}$  which is the median of the data in Fig. 5 and explore the consequences.

#### 6.4 True MOND fits

The fits to the rotation curves of the sample have been done again but now for a fixed value of  $a_0$  equal to the median of the sample. It appears that for the eight galaxies belonging to the trend subsample, for which  $a_0$  in Fig. 5 ranges between 0.9 and  $1.6 \cdot 10^{-8} \text{ cm s}^{-2}$ , one can in general make a reasonable fit, having only M/L as a free parameter. There are in some cases small systematic differences, but these could be explained by inherent systematic uncertainties associated with the derivation of the rotation curve from the observed velocity field. Even the most massive galaxy, NGC 2841, now at a distance of 14.1 Mpc, seems to be consistent with MOND.

The four outliers in Fig. 5 have been considered in more detail. MOND fits to the rotation curves of these galaxies using  $a_0 = 1.3 \cdot 10^{-8} \text{ cm s}^{-2}$  are presented in Fig. 6. Obviously, in all four cases there is a clear and systematic deviation from the observed data. For NGC 2998 and 3198 the fit in the inner regions is too low by 10 to 20  $\text{km s}^{-1}$  and the fit in the outer regions is too high by the same amount. For NGC 5585 and NGC 3109 the deviation is in the opposite sense, the fit is too high in the inner regions and too low in the outer regions. Considering the relations involved it is clear that MOND prefers a smaller distance to the first two galaxies and a larger distance to the latter two. Therefore, to assess the seriousness of the misfit it has been investigated how far the fit can be improved by taking a more favourable distance.

#### 6.5 MOND?

As a limit to what is possible the three sigma deviation has been taken from the nominal distance quoted in Table 1. This three sigma needs some explanation for the individual cases. At first NGC 3198 which has a (metallicity corrected) distance of 13.8 Mpc. The random  $1\sigma$  error amounts to 0.5 Mpc but the systematic error for an individual galaxy as determined by Freedman et al. (2001) is not immediately obvious. On page 54 of that paper, second equation, the systematic error is given as the quadratic sum of the contributing errors of (1) the zeropoint LMC PL relation, (2) the metallicity, (3) the photometric zero point and (4) of aperture correction for bias, crowding, background etc. The quoted numbers for errors (1) to (4) are 5%, 3.5%, 3.5%, and 0 to 5% (we use 2.5%) respectively. Adding in quadrature gives the systematic error for an individual galaxy of 7.5% and thus 1.03 Mpc for NGC 3198. The total, systematic plus random error for NGC 3198 then amounts to 1.14 Mpc ( $1\sigma$ ) and 3.42 Mpc ( $3\sigma$ ) and the more favourable distance at the  $3\sigma$  level is then 10.38 Mpc. This is a conservative error since the WMAP measurements (Spergel et al. 2007) indicate that the Hubble constant determined by Freedman et al. is in reality more accurate than quoted. For NGC 3109 the Cepheid distance of  $1.36 \pm 0.10$  Mpc is used (Musella et al. 1997), but as noted before, recent observations by Soszynski et al. (2006) suggest the Cepheid distance to be at  $1.30 \pm 0.04$  Mpc. Considering these numbers the plus three sigma limit has been put at 1.6 Mpc. NGC 2998 has no determined Cepheid distance. Yet the galaxy is relatively far away at a Hubble distance of 67.4 Mpc. The error in the distance is taken as the quadratic sum of the errors of the Hubble

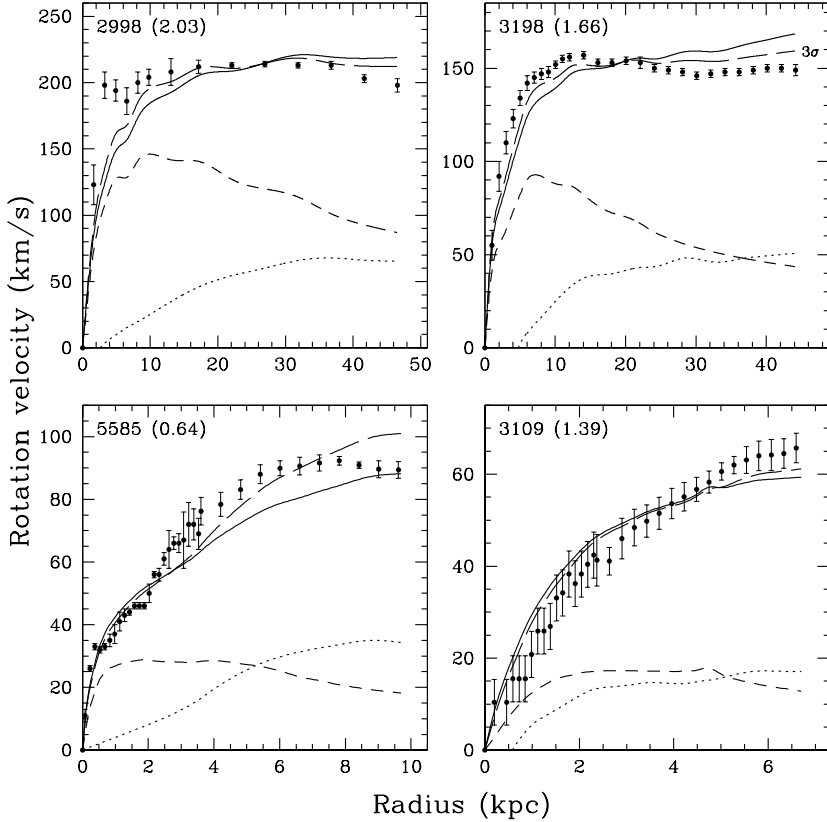


**Figure 6.** One parameter MOND fits to the rotation curves of four galaxies for which the two parameter fit generates the most deviating  $a_0$  value; using a fixed  $a_0$  of  $1.3 \cdot 10^{-8} \text{ cm s}^{-2}$ . The full drawn line is the best fit, while the long dashed line indicates the fit for a  $3\sigma$  more favourable distance. The short dashed and dotted line are the disc and gas contributions respectively. In principle, MOND should be able to explain the rotation curves for all galaxies with a universal value of  $a_0$ ; which is obviously not possible. Between brackets just after the galaxy name is the fitted value of  $(M/L)_{\text{obs}}^R$  using the nominal distance.

constant (for  $1\sigma$   $5 \text{ km s}^{-1}$  per Mpc) and a possible deviation from a regular Hubble flow ( $250 \text{ km s}^{-1}$  at  $1\sigma$ ). A three sigma more favourable distance is then at 50.6 Mpc instead of the nominal 67.4 Mpc. For NGC 5585 there is a Hubble distance of 6.2 Mpc and there is a distance of 8.7 Mpc from an analysis of the brightest stars (Drozdovsky & Karachentsev 2000) which the authors qualify as “somewhat uncertain”. Anyway, for the present this 8.7 Mpc is, admittedly somewhat arbitrary, considered as the  $3\sigma$  upper distance limit.

For the more favourable limiting distances the MOND fits using the median value of  $a_0$  are given by the long dashed lines in Fig. 6. Compared with the fits using the nominal distance for the galaxies NGC 2998, 3198, and 3109 there is some improvement. As can be noticed, the rotation curve of NGC 2998 is sampled by a limited number of points because the galaxy is distant. The deviation of the fit from the data remains systematic and significant but only for a handful data points. For NGC 3198 the difference between the fit and data is systematic and large for the majority of a large number of independent rotational data points although the fit can be made less deviant by taking an outmost smaller distance. NGC 3109 also shows a systematic deviation over the whole radial extent. Yet the errors on the rotational points are considerable which leads to a difference which is significant but not extreme. For NGC 5585 the fit can be improved considerably by taking an acceptably larger distance; the correspondence between the fit and data is then comparable to the fit when taking  $a_0$  as a free parameter (Fig. 4). That fit, however, was already noted to be not so good, certainly when compared with the fit using DM. For the adopted median value of  $1.3 \cdot 10^{-8} \text{ cm s}^{-2}$  for  $a_0$  one

can then conclude that for MOND there is a small problem for NGC 5585, a problem for NGC 2998 and NGC 3109 and a serious problem for NGC 3198. In second instance a universal value for  $a_0$  of  $0.9 \cdot 10^{-8} \text{ cm s}^{-2}$  has been investigated. The MOND fit then improves for NGC 3198 and as demonstrated by BPRS, putting the galaxy  $2\sigma$  closer makes the fit marginally consistent with the data. Also the MOND fit for NGC 2998 improves markedly, but the fit for NGC 3109 and NGC 5585 becomes considerably worse. However, for this value of  $a_0$  NGC 2841 gives serious and significant problems (see BPRS).

When  $a_0$  is allowed as a free parameter a large range of values is found. That is essentially the reason for the subsequent finding that it is not possible to make acceptable MOND fits for all galaxies for any value of  $a_0$ . This does not add to the credibility of the theory.

## 7 ADIABATIC CONTRACTION

Galactic dark matter halos formed in the universe by cumulating matter cannot preserve their original density distribution. The baryonic mass component within a halo will collapse mainly dissipational and in doing so pulls dissipationless dark matter to the centre. Thus when finally a galaxy has formed its dark matter halo has a different radial distribution compared to distributions predicted by pure CDM cosmological simulations. A prescription is needed to relate the DM profiles of the present sample of galaxies to those of the pre collapsed galaxies.

### 7.1 Standard Adiabatic Contraction

Such prescriptions or mechanisms have been designed and investigated in several studies. The original specific and comprehensive work on this matter is by Blumenthal et al. (1986). They consider the fate of a halo with an original homogeneous mixture of dissipationless DM and baryonic matter. Such a halo contracts when the baryons fall in dissipatively. When the baryonic mass fraction ( $F$ ) is small and for the simplifying approximation that the orbits of dissipationless halo particles are circular, the quantity  $rM(r)$  is an invariant, where  $M(r)$  is the total mass within radius  $r$ . For this situation the orbits of halo particles essentially change adiabatically and the mechanism has been named Adiabatic Contraction (AC).

Assume that the initial spherically symmetric cumulative mass distribution  $M_i(R)$  at initial radius  $R$  is a mixture of collisionless DM ( $M_{i,\text{dm}}(R)$ ) and fraction  $F$  of baryonic matter,  $F = M_{i,\text{bar}}/M_i$ . The baryons cool and fall into a final galaxy cumulative mass distribution  $M_{\text{gal}}(r)$  at final radius  $r$ . Then the adiabatic invariant implies that

$$r [M_{\text{gal}}(r) + M_f(r)] = RM_i(R) \quad (9)$$

with the continuity condition of

$$M_f(r) = (1 - F)M_i(R) \quad (10)$$

Here  $M_f(r)$  is the final DM cumulative mass at final radius  $r$  contracted from the initial cumulative distribution  $M_{i,\text{dm}}(R)$ . In practice, for an initial distribution  $M_i$ , for every initial radius  $R$  one can solve equations (9) and (10) to get the final radius  $r$ . Converting to rotational velocities, the final rotation  $v_f(r)$  is then given by

$$v_f(r) = \sqrt{\frac{(1 - F)M_i(R)}{r}} = \sqrt{\frac{M_{i,\text{dm}}}{r}} = v_{i,\text{dm}}(R) \sqrt{\frac{R}{r}} \quad (11)$$

This AC prescription is not straightforward; the final distribution and rotation curve has to be calculated for every radius separately using given but not always simple cumulative mass distributions. From now on we shall refer to the mechanism described above as the standard AC model.

Blumenthal et al. explore this standard AC for various cored dark matter and disk distributions. In general an original pseudo isothermal mass distribution changes into a distribution which is much more centrally concentrated. Therefore assuming both, that the standard AC is correct and original halos are pseudo isothermal, it is unlikely that present day halos have strictly pseudo isothermal profiles.

### 7.2 Modified AC

The matter of AC on itself has been re-investigated by Gnedin et al. (2004). They perform and analyse numerical simulations mainly of clusters, including a.o. gas cooling, dissipation, and star formation. In general the result is that standard AC overpredicts the concentration of DM in the inner regions of the clusters. Gnedin et al. propose a modified AC prescription, which they tested to give a good representation of the density profiles of simulated clusters. The proposed modification is to use the quantity  $rM(\bar{r})$  as the invariant instead of  $rM(r)$ . Here  $\bar{r}$  is the orbit averaged radius of an isotropic distribution which can be approximated fairly well by

$$\bar{r} = Ar^w \quad (12)$$

over a wide range of radii with  $A \approx 0.85$  and  $w \approx 0.8$ . Equations (9), (10), and (11) then change into

$$r [M_{\text{gal}}(\bar{r}) + M_f(\bar{r})] = RM_i(\bar{R}) \quad (13)$$

$$M_f(\bar{r}) = (1 - F)M_i(\bar{R}) \quad (14)$$

and

$$v_f(\bar{r}) = v_{i,\text{dm}}(\bar{R}) \sqrt{\frac{\bar{R}}{\bar{r}}} \quad (15)$$

For the single galactic halo they investigated the correspondence between the simulation and the modified prescription was less satisfactory.

### 7.3 Testing AC

Later on Choi et al. (2006) also investigated these matters. Amongst others 3D N-body simulations have been carried out of galactic DM halos with an isotropic velocity distribution. Various galaxy formation scenarios and DM halo concentrations have been considered representing the different results of cosmological simulations. Choi et al. find that for NFW halos the standard AC prescription gives, on average, halo rotations at  $R = 2.2h_{\text{disc}}$  which are 6% too large. For Gnedin's modified AC prescription with  $A = 0.85$  and  $w = 0.8$  the correspondence between the halo rotations of theory and of simulations is satisfactory, in general. On the other hand it is not possible to reconcile the structure of the emerging cored halos with predictions of any theory. Using the standard AC the halo rotations at  $R = 2.2h_{\text{disc}}$  are about 20% too large compared to that of the simulated halos. Considering masses this gives errors larger than 40%, a huge number. In fact, this means that the results of Blumenthal et al. concerning pseudo isothermal cored halo distributions are not correct, in retrospect.

The AC theory works better for initially more concentrated halos. As Choi et al. argue, this can be explained by the distribution of the orbits. For isotropic halos, in order to be less concentrated, a larger fraction of more radial orbits is needed. Therefore the assumptions underlying standard AC become less adequate for less concentrated dark halos. Consequently one may expect a worse correspondence between the predictions of standard AC and real contraction for shallower halo distributions. This also explains the results of Jesseit et al. (2002) that standard AC works well for Hernquist (1990) halos which are even more concentrated than NFW halos.

### 7.4 The AC which has been used

In the next section rotation curve decompositions will be considered for NFW halos. Such halo shapes are predicted by cosmological CDM formation scenarios. Subsequent galaxy formation will therefore make the original density profile more concentrated and an AC mechanism is needed to relate the original profile to the present day halo distribution and rotation curve. In accordance with the discussion above the modified AC prescription will be used. In Sect. 9, following the results of Sect. 8, cored pseudo isothermal halos are considered. The resulting halo rotation curves from the

rotation curve decomposition procedure have been adiabatically de-contracted in order to generate pre baryonic collapse density profiles. But how should one do this de-contraction when the standard procedure produces rotations which are off by 20% and even the modified AC is not correct? As suggested by Gnedin et al.'s analysis, AC can be made gentler by using the  $\bar{r}$  of Eq. (12). We have investigated if AC can be made even gentler by changing the values of  $A$  and  $w$ . It appears that for  $w = 0.5$  instead of 0.8 the AC rotations of the halo at  $R = 2.2h$  can be lowered by the amount to bring them in agreement with the simulation results of Choi et al. Therefore, to do the adiabatic de-contraction of cored halos the invariant  $rM(\bar{r})$  is used with  $\bar{r} = 0.85 r^{0.5}$ ; and it is checked if indeed the de-contracted halo rotation is in agreement with a cored distribution. This procedure is somewhat artificial, but until more sophisticated AC methods become available, it is the best one can do.

## 8 NFW-CDMA-AC FITS

### 8.1 A one parameter NFW halo

For an NFW halo the density distribution takes the form

$$\rho_{\text{NFW}} = \frac{\rho_i}{(R/R_s)(1 + R/R_s)^2} \quad (16)$$

where  $R_s$  is a characteristic radius and  $\rho_i$  is related to the density of the universe at the time of collapse. The rotation curve  $v_{\text{NFW}}$  following from this distribution is

$$v_{\text{NFW}} = 2.15 v_{\text{max}} \sqrt{\frac{R_s}{R} \ln\left(\frac{R}{R_s} + 1\right) - \frac{R_s}{R + R_s}} \quad (17)$$

where the maximum rotation  $v_{\text{max}}$  is reached at a radius of  $2.16R_s$ . When a certain cosmology is chosen the structural parameter becomes related to the total mass of the halo. Following Bottema (2002) we assume the current concordance model for the cosmology: a low density CDM universe with flat geometry, called CDMA with  $\Omega_0 = 0.25$ ,  $\Lambda = 0.75$ , and a Hubble constant of  $75 \text{ km s}^{-1}$  per Megaparsec. For that cosmology Navarro et al. (1997) relate the parameter  $M_{200}$  to  $v_{\text{max}}$  in their Fig. 7. Some manipulation with equations leads to the following relation between  $R_s$  and  $v_{\text{max}}$

$$\frac{R_s}{[\text{kpc}]} = 0.0127 \left( \frac{v_{\text{max}}}{[\text{km s}^{-1}]} \right)^{1.37} \quad (18)$$

such that when Eqs. (17) and (18) are combined there is only one free parameter ( $v_{\text{max}}$ ) left for the dark halo. One may relate the present parameters to that of the concentration parameter  $c$ , often appearing in the literature by

$$c = 55.74 \left( \frac{v_{\text{max}}}{[\text{km s}^{-1}]} \right)^{-0.2933} \quad (19)$$

of which the value will be given as well.

One way to proceed when making NFW halo decompositions, is to maintain two free halo parameters and do a least squares fit to determine e.g.  $c$  and  $V_{200}$  (de Blok et al. 2001; Navarro 1998). For each galaxy a data point is generated in the  $c, V_{200}$  plane and the distribution of points in this plane can be compared with the distribution generated by numerical simulations for various cosmologies. For an observed rotation curve which is close to solid body, however,

problems will occur. An NFW halo has  $v_{\text{halo}} \propto \sqrt{R}$  in the inner regions. When such a functionality is fitted to  $v_{\text{obs}} \propto R$  the fit parameters get forced into an extreme region of parameter space:  $c$  and  $V_{200}$  diverge to a small and large value respectively. One then has a situation where a small galaxy is embedded in a gigantic dark halo. The diverged structure of this halo is barely related to the galaxy under investigation and a comparison with numerically generated dark halos is not appropriate. In practice one circumvents this divergence by setting artificial bounds to e.g.  $c$  (see de Blok et al. 2001).

Since the cosmology has now become better established, constraints on NFW halos like those given by Eq. (18) can be used. This is fortunate because then the degeneracy can be relieved between disc mass and dark halo contribution for a fit to an observed rotation curve. In addition, a diverging fit to an inner solid body rotation curve for small galaxies does not appear any more. For the remainder of this section NFW fits will be made to rotation curves using two parameters (M/L ratio and  $v_{\text{max}}$ ) for systems without bulges and three parameters (+ M/L ratio of the bulge) for galaxies with bulges. In practice the constraining relation (18) is an average and cosmological simulations display a certain scatter around the relation. If one investigates only one galaxy this scatter has to be taken into account by considering the probability that the halo properties of that particular galaxy deviate from the average. But, for a collection of systems, as presently, an appearing systematic deviation from the average relation is sufficient to demonstrate an inconsistency.

### 8.2 Fitting the rotation curves (with AC)

Cosmology provides the constraint which is badly needed, but not without a trade-off, namely the necessity to apply an AC procedure. This procedure has been applied to the halos of the sample of galaxies. For a certain M/L ratio of disc (and bulge) the radial cumulative mass profile of the baryonic component has been calculated from the photometric and H I density radial profiles. An NFW halo rotation curve parameterized by the value of  $v_{\text{max}}$  is then contracted to a new rotation curve which cannot be described by an analytical function any more. Furthermore, the shape of the curve is different for each different M/L ratio and obviously a straightforward least squares fitting method cannot be applied. Instead, the only way to proceed is by generating  $\chi^2$  difference values in the plane of the parameters M/L and  $v_{\text{max}}$  and searching this plane for the minimum  $\chi^2$  value. When a bulge is included the plane changes into a cube, of course, with the additional parameter the M/L ratio of the bulge. These procedures have all been performed and the final fits to the rotation curves are presented in Figure 7 and numerical values in Table 6. A few remarks before we investigate the fits. The value of the halo's maximum rotation  $v_{\text{max}}$  given in Table 6 applies to the original NFW halo including the mixed in baryonic fraction. One can calculate the maximum rotation of the DM component only by  $v_{\text{max}}^{\text{h, dm}} = \sqrt{1 - F_{200}} v_{\text{max}}^{\text{h, tot}}$  where  $F_{200} = M_{\text{bar}}/M_{200}$  also given in Table 6. The values of  $R_c$  and  $c$  follow directly from that of  $v_{\text{max}}$  by Eq's (18) and (19). Quoted errors have been inferred by taking the same fractional error as generated by the standard Marquard least squares fitting of a non contracted NFW halo. For NGC 7331 the disc contribution has

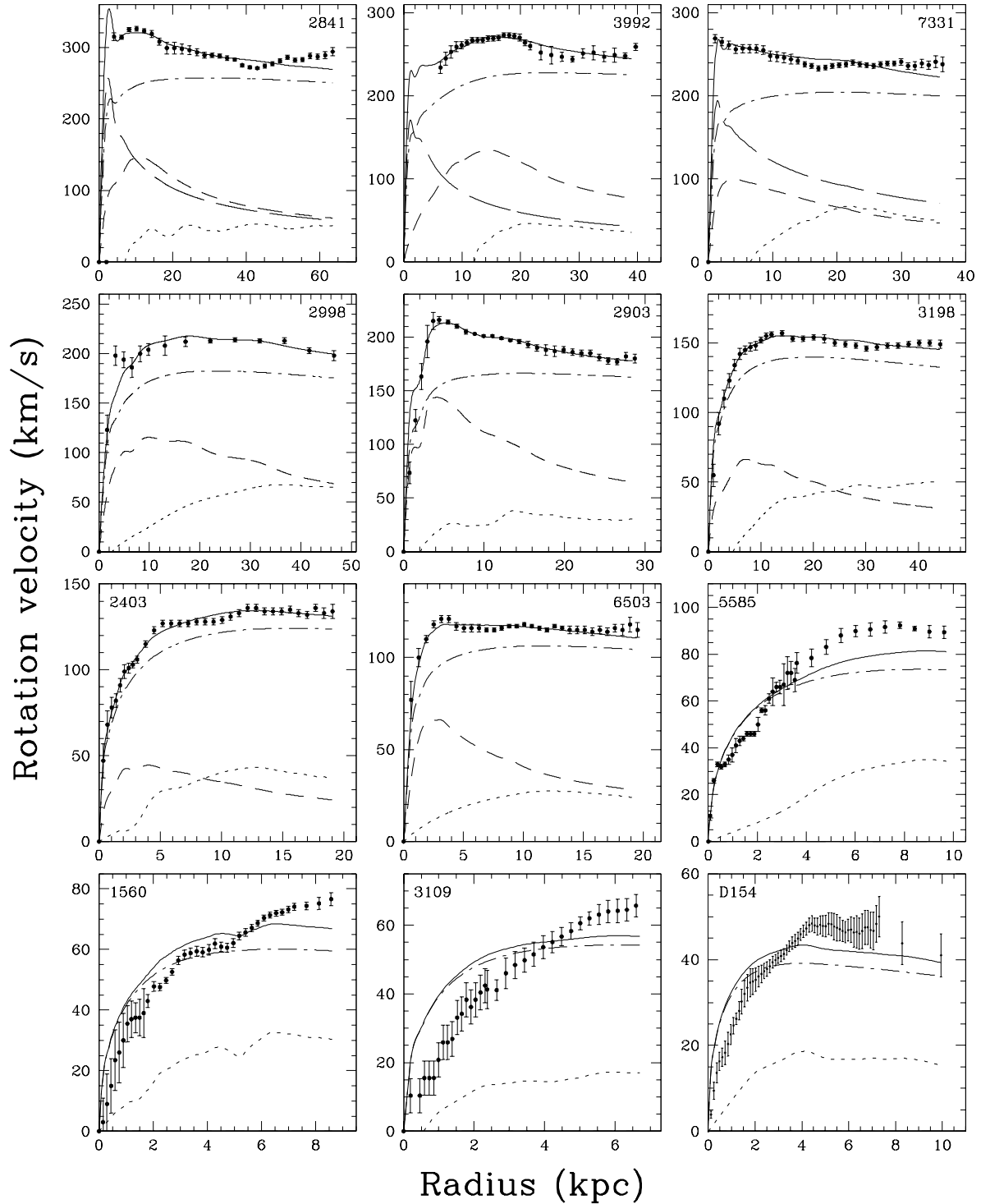


**Figure 7.** Fits to the observed rotation curves for NFW-CDMA dark halos including the appropriate process of adiabatic contraction. For the 8 most massive galaxies an adequate representation of the observed rotation can be achieved, though in some cases only for unrealistically small  $M/L$  ratios. For the 4 least luminous galaxies an NFW halo is clearly inconsistent with the observations even for a most favourable situation, as presented, where the luminous contribution has diverged to zero.

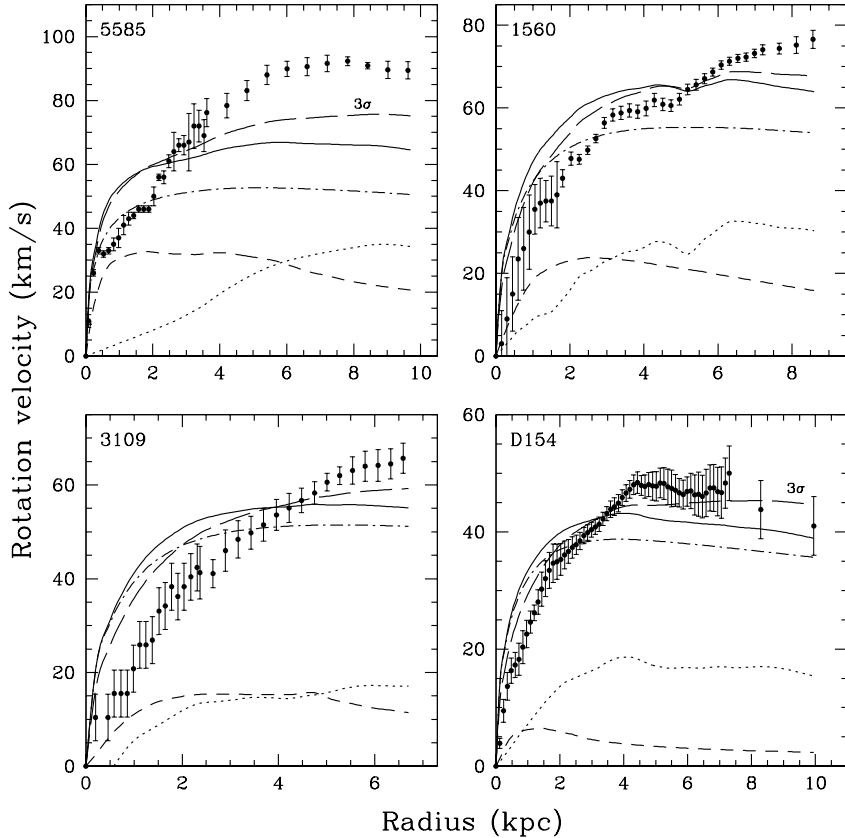


**Figure 8.** NFW-CDMA-AC fits to the rotation curves of the four least massive galaxies, using a realistic yet moderate M/L ratio for the disc. The discrepancy between fit and data then becomes larger compared to the situation without luminous matter, as in Fig. 7. Full drawn lines indicate the best fit, the dotted, dashed and dash-dot lines are for the gas, disc, and dark halo contributions respectively. In addition the fits for  $3\sigma$  less concentrated dark halos are given by the long dashed lines. Even for such an extreme deviation from the average properties the mismatch remains.

to be small, but is poorly constrained. It has been fixed at the low value suggested by the observed stellar velocity dispersions (Bottema 1999).

As can be seen in Fig. 7, for the more massive galaxies the fits are generally very acceptable and not worse than the maximum disc or MOND-like fits. There is, however, a significant difference when comparing the NFW fits with the previous ones. The disc is forced to a contribution which is substantially lower than the maximum possibility, in line with the conclusions of Dutton et al. (2005). This results in M/L ratios which are lower than the maximum disc and MOND values. Considering the galaxies with observed stellar velocity dispersions (excl N7331) the maximum contribution of the disc rotation to the total rotation is 54%, 42%, and 55% for NGC 2998, 3198, and 6503 respectively. Such values are at, or just below the lower limit inferred from the observed dispersions.

Comparing the fitting results with those obtained without the AC procedure one can note the following. For the more massive and certainly the more concentrated galaxies the effect of AC on the halo RC is more pronounced in the sense that the halos become more concentrated. Which is obvious, of course. For the smaller galaxies and the more so for those with only a minimal disc the AC effect is small. The gas mass distribution is relatively extended and has as such only a limited influence on the contraction. In general, when AC has been included the contribution of the luminous components becomes even smaller than it already was for NFW halos without AC. The bulge rotations are, on average, an extra 20% lower and the disc rotational contributions  $\sim 10\%$  lower.

### 8.3 Disagreement for small galaxies

As can be readily noticed, for the less massive galaxies with  $v_{\max} \lesssim 100 \text{ km s}^{-1}$ , the fits are not compatible with the data. There is no way the deviations can be explained by uncertainties or errors in the observed rotation. What can be noted as well is that the fits force the M/L ratio to zero. If instead a reasonable M/L ratio is adopted, the discrepancy between fit and data becomes even worse. This has been investigated by making extra NFW-AC fits for the four least massive galaxies assuming an M/L ratio which is modest in any way. For that we assume  $(M/L)_{\text{epc}} = 1.0$  following a.o. from stellar velocity dispersion observations and which is roughly half the value for a maximum disc contribution. The result is displayed in Fig. 8 and as can be seen, the correspondence between best fit and the data becomes even worse compared with the M/L = 0 case. Two effects contribute to this deterioration. At first the addition of a stellar contribution, but secondly, because of that, the halo density becomes slightly more concentrated by an increased AC effect.

### 8.4 Shallower NFW halos

The possibility has been explored that by some chance these four galaxies have formed in dark halos which were extremely shallow. Considering the Navarro et al. (1997) halos, which have been used in the present fitting procedure, Bottema (2002) derives a compromise value for the  $1\sigma$  scatter in  $\ln(c)$  of 0.25 based on the analyses of Bullock et al. (2001) and Jing (2000). This value of the scatter appears to be exactly equal to the value found by Macciò et al. (2008) for

relaxed halos resulting from later, more sophisticated simulations. That scatter value can thus be used with some confidence. It is easy to demonstrate that a scatter in  $\ln(c)$  translates in exactly the same scatter in  $\ln(R_s)$  and so in a scatter to the coefficient 0.0127 in Eq. (18). A shallower halo by  $1\sigma$  then gives a coefficient of 0.0163 and by  $3\sigma$  of 0.027; for the same  $v_{\max}$  the associated  $R_s$  is then increased. For a  $3\sigma$  less concentrated halo fitting results are displayed in Fig. 8 as well. It can be noticed that the correspondence between data and best fit improves, but the discrepancy remains large. Values of the concentration parameter  $c$  for the nominal fits are given in Table 6 and amount to an average of 17.5 for the four least luminous galaxies. For  $3\sigma$  less concentrated halos the value of  $c$  is then a factor 2.12 less or approximately 8. Making a two parameter NFW halo fit to the rotation curves can generate acceptable fits, but concentration parameters then decrease to a value below 4 while the core radius parameter  $R_s$  ends up above 12 kpc and the mass-to-light ratio tends towards zero. This is a situation of a small galaxy embedded in a giant DM halo, as discussed above.

Using the Millennium Simulation Neto et al. (2007) establish that NFW halos appear to be shallower than the halos investigated by Navarro et al. (1997). A relation is found for NFW halos of  $c = 5.26 (M_{200}/[10^{14}h^{-1}M_{\odot}])^{-0.10}$  for  $M_{200} \gtrsim 10^{12}M_{\odot}$  which is compatible with the relation  $c = 5.6 (M_{200}/[10^{14}h^{-1}M_{\odot}])^{-0.098}$  for  $M_{200} \gtrsim 10^{10}M_{\odot}$ , so for smaller halos, as derived by Macciò et al. (2007). The relation by Neto et al. can be converted in a  $R_s$  versus  $v_{\max}$  relation as in Eq. (18) using  $h = 0.75$ :

$$\frac{R_s}{[\text{kpc}]} = 0.0197 \left( \frac{v_{\max}}{[\text{km s}^{-1}]} \right)^{1.37} \quad (20)$$

thus having the same exponent as in Eq. (18) but a larger factor of 0.0197 instead of 0.0127, expressing that the halos are indeed shallower. Then halos of the shape of Neto et al. (2007) are equal to the NFW halos of Eq. (18) but shallower at a deviation of  $1.7\sigma$ . If such fits were to be plotted in Fig. 8, these would then be between the displayed nominal and  $3\sigma$  fits. In fact, fits of Neto et al. halos, being  $1\sigma$  more shallow than their average would nearly coincide with Navarro et al. (1997) halos which are  $3\sigma$  shallower. As can be seen, such fits are very deviant from the observations; the chance of finding four galaxies which are shallower by  $1\sigma$  from the average amounts to 0.00063. It appears that the value of the concentration slightly depends on the exact cosmology (Macciò et al. 2008; Ludlow et al. 2014) and now seems to swing backwards from the shallow Neto et al. (2007) determination to a larger concentration. Anyhow, the fitting possibilities allowed by different cosmologies and simulation techniques should be sufficiently well illustrated in Fig. 8.

The standard CDM halo formation scenarios predict halos with an NFW profile on all scales. Consequently that scenario is not consistent with observed rotation curves of less massive galaxies, as mentioned already in the introduction, and demonstrated here rather dramatically. It is even in conflict with RC analyses for intermediate galaxies because of the predicted too low disc contributions. A more general and extended discussion of these matters is deferred to Sect. 10.

## 9 EQUAL MASS-TO-LIGHT RATIO FITS

Under normal galactic conditions, the IMF seems to be universal or at least barely dependent on metallicity or star formation rate (Kroupa 2001, Bell & de Jong 2001). Because the M/L ratio is directly related to the IMF one expects this ratio to be universal too, at least when properly corrected for extinction and population effects. Therefore rotation curve decompositions will be made assuming an equal  $(M/L)_{\text{epc}}$  for all the galaxies.

### 9.1 The value of the M/L ratio

What value should one use? It certainly has to be smaller than the smallest maximum disc and maximum bulge values displayed in Fig. 3, or else some rotation curves will rise above the observations. The appropriate value for any disc can, in principle, be derived from measured stellar velocity dispersions. Unfortunately such a derivation is not straightforward. At first, because the observed stellar velocity dispersions come with a considerable error; the M/L ratio is proportional to the square of the dispersion and hence M/L even has a larger uncertainty. Secondly, in order to derive the mass-to-light ratio, assumptions have to be made for the scalelength to thickness ratio ( $h/z_0$ ) of a disc, the ratio of vertical to radial velocity dispersion, and absorption corrections. For four galaxies of the sample values are given in Table 7, all derived for appropriate disc parameters and conditions. Excluding NGC 7331, which has the most uncertain value because its disc light is so dominated by the bulge, an average  $(M/L)_{\text{epc}} = 1.04 \pm \sim 0.3$  is found. Considering this number and the above-mentioned requirement to have an  $(M/L)_{\text{epc}}$  below the lowest maximum disc/bulge numbers, a plausible value for the universal  $(M/L)_{\text{epc}}$  of 1.0 has been chosen. It could equally well be 0.9 or even 1.1 or 1.2 yet for now the consequences will be explored for a reasonable equal value for all discs and bulges of the sample of galaxies.

### 9.2 Fitting the rotation curves

Using a pseudo isothermal halo and  $(M/L)_{\text{epc}} = 1.0$  for all components, the resulting fits are presented in Fig. 9 and Table 8. The agreement between model curves and the data points is excellent in general. The exception being the outermost velocities of DDO 154, which don't fit in any case. In general the discs are sub maximal which is a logical consequence of an assumed M/L ratio resulting from observed stellar velocity dispersions (Bottenga 1993; Martinsson et al. 2013). However, for the cases where the disc contribution should be larger because a specific disc feature is clearly expressed in the observed rotation curve, the disc contribution is indeed larger, for example for NGC 2903 and NGC 5585. Moreover, the bulges give a dominant contribution to the rotation, which they should do in order to keep the rotation flat near the centre. It can be concluded that one universal M/L ratio provides the possibility to make excellent fits to observed high quality and extended rotation curves. Contrary to maximum disc fits there is a physical basis for the adopted M/L ratio and it can be calculated for every galaxy a priori. Considering the results just mentioned, the argumentation can be turned around. If there is indeed a

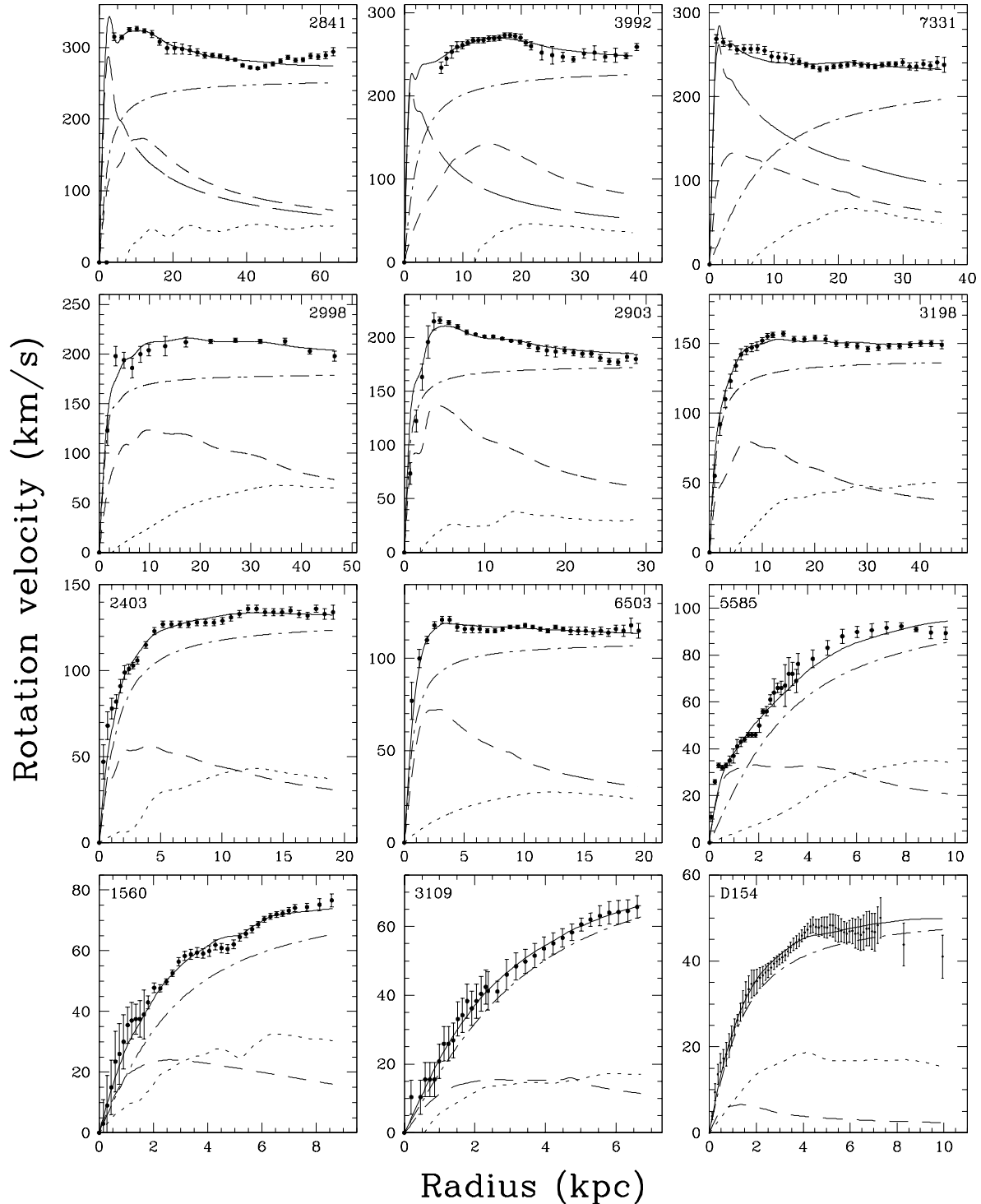


**Figure 9.** Fits to the observed rotation curves for one universal value of the  $M/L$  ratio ( $(M/L)_{\text{epc}}^R = 1.0$ ) and pseudo isothermal dark halo. There is an excellent agreement between the model and data. For this fit procedure the rotational contribution of the luminous components is set a priori by the amount of light and the colour; in general discs appear to be sub maximal and bulges maximal.

universal  $(M/L)_{\text{epc}}$  ratio what can its value be by only investigating the rotation curve fitting? Making it larger than  $\sim 1.1$  lifts the RCs above the observations for NGC 2841, 7331, and 5585. On the other hand, making it smaller than  $\sim 0.9$  the fit for NGC 2903 gets considerably worse. Thus,

in retrospect, the choice of  $(M/L)_{\text{epc}} = 1.0$  was appropriate, though admittedly, we iterated once on this matter and increased the number from 0.9 to 1.0.

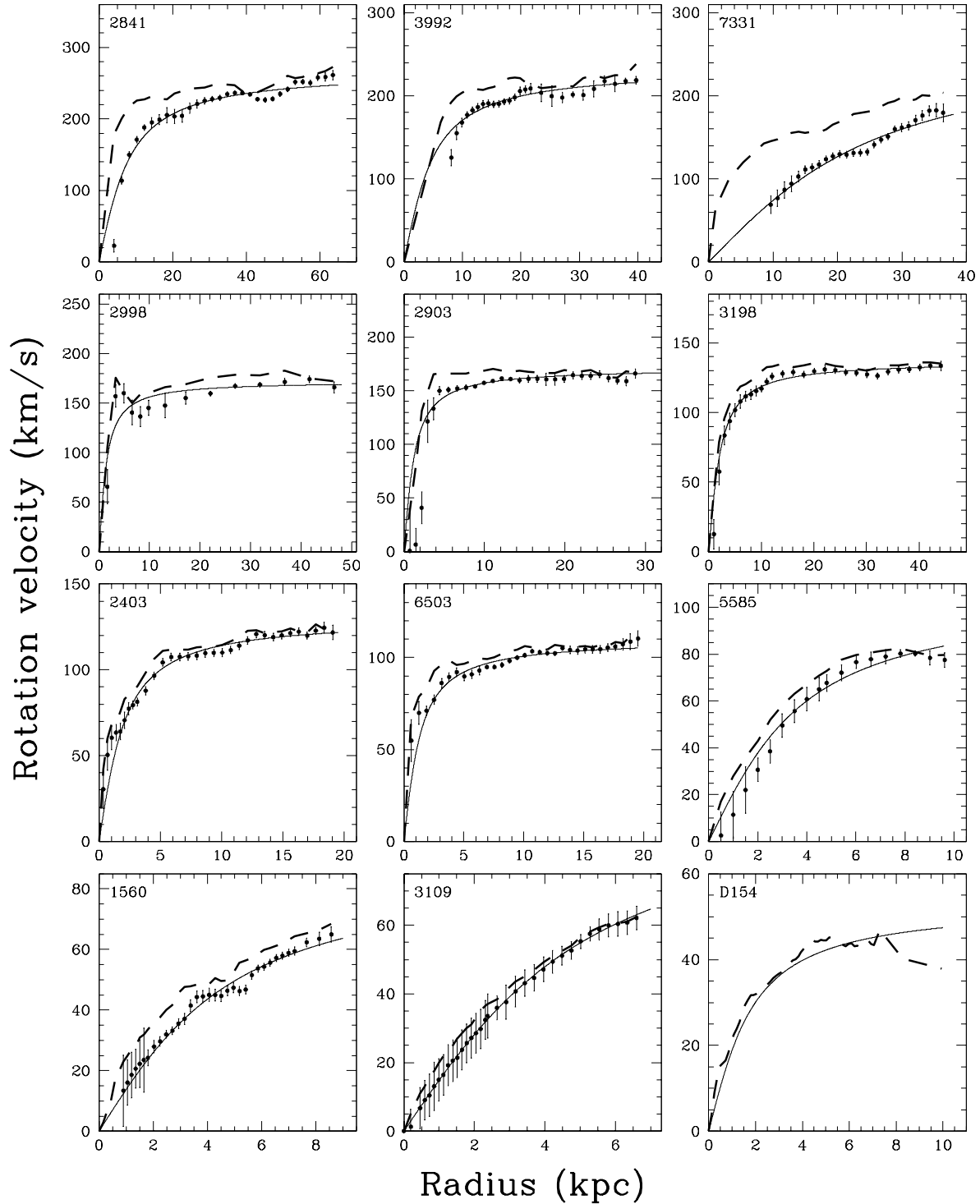


**Figure 10.** Dark matter rotation curves which result after subtraction of the rotation of the luminous components, all with equal universal  $M/L$  ratio, and of the rotation of the gas. The dashed line gives the result derived directly from the observations, the points represent the adiabatically de-contracted dark halo rotation, resampled to the original radial positions and with appropriate errors. To these points a fit is made of a pseudo isothermal halo given by the full drawn line. For DDO154 the data points have been omitted to avoid confusion; for that case the de-contraction is very small.

### 9.3 Pure dark matter

Following the findings and discussion above a more fundamental approach can be taken to derive the contribution of the dark halo. Assuming that one knows for every galaxy what the contribution of the luminous component is, taking  $(M/L)_{\text{epc}} = 1.0$ , one can simply subtract the luminous contribution from the observed rotation curve and retain the rotation of the dark halo only. This has been done for the sample and the resulting halo rotation curves are given in Fig. 10 by the dashed lines. In this way a nice impression is obtained of pure dark matter. Fits of any functionality can be made to these dark halo rotation curves. For the specific pseudo isothermal halo functionality of Eq. (6) nearly identical results would have been obtained as for the combined fit performed to the total rotation curves as tabulated in Table 8. To relate the data to the original, pre galaxy formation dark halos the rotation curves of the halo have to be adiabatically de-contracted. Using the scheme described in Sect. 7 this has been done under the assumption that the original dark halos are pseudo isothermal. The result is given in Fig. 10 too, where the de-contracted halo RCs have been re-sampled to the original radial positions and the errors have been copied from the contracted halo rotation curves. Fits of a pseudo isothermal functionality have been made to these rotational data points, being very acceptable (except for DDO 154 again) and resulting fit parameters  $R_c$  and  $v_{\text{max}}$  are given in Table 8.

The derived halo core radii have been plotted versus halo maximum rotation in Fig. 11, both for the direct fit to the total observed RC and for the fit to the adiabatically de-contracted dark halos on itself. In general  $R_{\text{core}} \lesssim 4$  kpc and in first instance no clear correlation or trend seems visible. The process of adiabatic de-contraction makes the core radii larger, as expected, by some 30 to 100%, but the general appearance in Fig. 11 does not change significantly. For every galaxy the value of the core radius is rather specific and changes by more than 50% quickly give a disagreement between model and observed rotation curves. But this is only so for the employed fixed disc and bulge contribution at  $(M/L)_{\text{epc}} = 1.0$ . It might be investigated if changes of this M/L ratio for each galaxy, within the boundaries of the uncertainties, can stretch the possible range of fitted core radii, and if an equal value for all core radii for all galaxies is possible. Results of such an investigation will be presented in a future paper.

### 9.4 Other than pseudo isothermal halo densities

The investigation of the dark matter distribution for a universal M/L ratio has concentrated, so far, on a pseudo isothermal radial functionality and can as such give a consistent explanation of the observations. But how about other DM radial functionalities and specifically that of an NFW halo? To investigate this for the sample of galaxies the halo RCs obtained after subtracting the baryonic components with  $(M/L)_{\text{epc}} = 1.0$  have been adiabatically de-contracted using  $w = 0.8$ , appropriate for NFW halos. Then there is a first problem for the three galaxies with bulges. For these the process of adiabatic de-contraction with  $w = 0.8$  is so severe that for the inner halves of the halo RCs non realistic decontractions are found. For the intermediate galaxies,

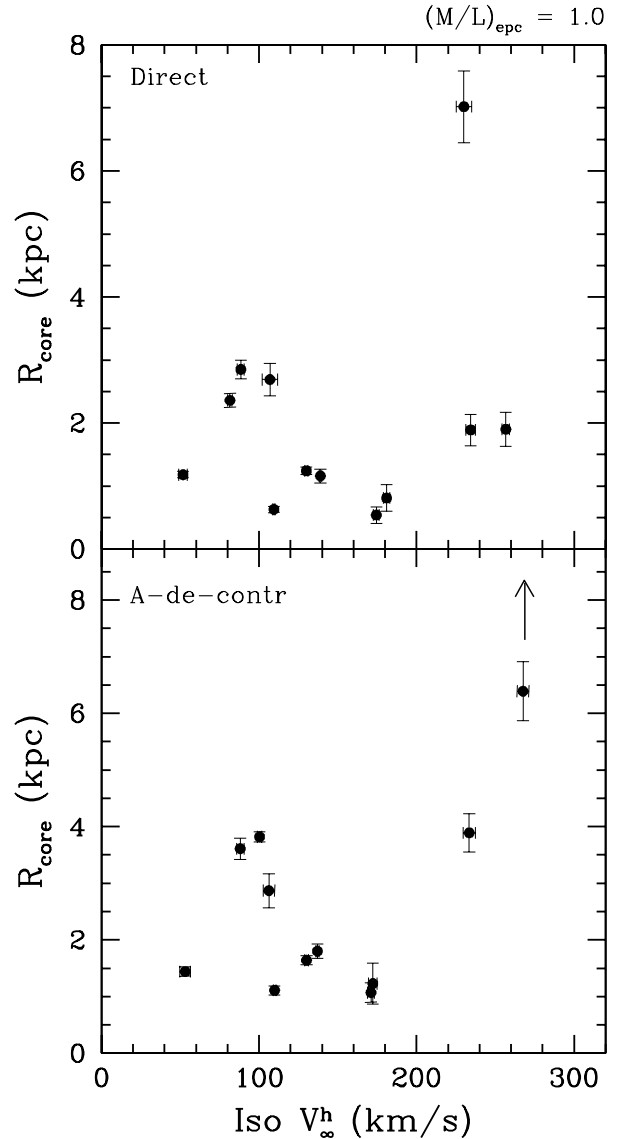


**Figure 11.** Core radius versus maximum rotation of the pseudo isothermal halo fit to the dark halo rotation curves in case of the adopted universal M/L ratio for the luminous components. *Top:* for the composite rotation curve fit, directly to the data as in Fig. 9. *Bottom:* for the fit to the dark halo which results after subtraction of the baryonic rotation and subsequent adiabatic de-contraction, as in Fig. 10. There is a moderate range of core radii, but no trend or correlation seems apparent. In the bottom plot the off-scale value for NGC 7331 is indicated by the arrow.

the decontraction works fine and in general a satisfactory fit of a two parameter NFW rotation curve (Eq. 17) can be made to the data. But there is nothing new. For example, let us consider the galaxy NGC 3198. The pseudo isothermal fitting procedure to the halo RC gives a good fit to the data over the range between  $2R_c$  and  $25R_c$ . Over that range of radii the value of  $\ln\rho/\ln r$  of the halo goes from -1.5 to -2. For the NFW fit procedure the fit is acceptable from  $R = 0.2R_s$  to  $3R_s$  and then  $\ln\rho/\ln r$  ranges between -1 to -2.5. So considering the radial functionality of the dark halo density there is in fact not much difference between a

pseudo isothermal and an NFW halo, and both can over a specific range of  $R/R_{c,s}$  describe the observations.

A difference between pseudo isothermal and NFW can only be noticed there where both differ. That is in the outer regions where for the NFW profile  $\ln\rho/\ln r$  goes to -3 while for a pseudo isothermal profile it cannot go below -2. Translated in RCs that means that in order to distinguish NFW from pseudo isothermal a maximum rotation and decline beyond has, or has not, to be observed. Inspection of Fig. 10 shows that (except for DDO154) the RCs of the halos continue to rise and consequently there is no evidence, at large radii, that an NFW profile is to be favoured over a pseudo isothermal profile.

Also in the inner regions the profiles differ. An NFW halo does not have a  $\ln\rho/\ln r > -1$  (the cusp) while for small radii a pseudo isothermal halo has  $-1 < \ln\rho/\ln r < 0$  (the core). For example the halo of the galaxy NGC 1560 has after adiabatic decontraction a  $\ln\rho/\ln r$  ranging from  $\sim -0.1$  to -1.7 which cannot be reconciled with the RC of an NFW halo. The rotational data points of the halo are simply too close to solid body rotation to be reconciled with  $v_{\text{rot}} \propto \sqrt{r}$  over the observed range of radii. Also for two other small galaxies, NGC 5585 and NGC 3109, it is not possible to fit an NFW two parameter RC to the halo data points. Therefore it can be concluded that under the assumption of a universal  $(M/L)_{\text{epc}}$  value of 1.0 an NFW radial density profile is not consistent with a considerable fraction of the galactic dark halos.

Burkert halos (Burkert 1995) combine the constant density (isothermal) inner core with an  $R^{-3}$  (NFW) functionality at large radii. Fits of the rotational functionality of such halos have been made to the A-de-Contracted halos of the sample as presented in Fig. 10. It appears that for the galaxies more massive than NGC 5585 the fits differ systematically from the data; in the inner and outer regions data lie above the fit while in the central regions it is the other way around. This is because a Burkert halo has a maximum rotation while for a good fit a radial section with nearly flat rotation is needed. For the small galaxies Burkert works well. This is easily explained because for these systems the rotation still rises, and the curve is fitted with the inner, constant density part of the Burkert halo. If also the M/L ratio were left as a free parameter, the fit would converge to a maximum disc situation. The then remaining halo is forced into the constant density inner section of the Burkert functionality and a better fit is achieved.

### 9.5 Tully-Fisher-like relations

To further investigate any physical correlations a few Tully-Fisher like relations have been put together. At first, in Fig. 12, the total baryonic mass is given as a function of the rotational velocity at the flat part of the rotation curve. The errors on the baryonic mass have been taken at 20%, which is estimated to be the combined uncertainty of absorption and population corrections and distance (see Sect. 10.3 for a discussion). To determine the error on  $v_{\text{flat}}$  an inspection by eye is made of the rotation curve in the outer regions. Fig. 12 displays an astonishingly good linear relation over  $2\frac{1}{2}$  orders of magnitude in galaxy mass. A fit of a straight line to the data points has been made, taking the errors in

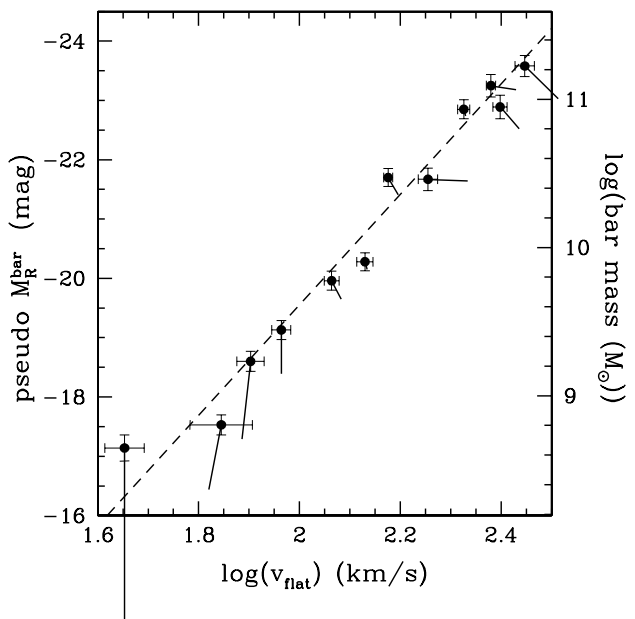


**Figure 12.** A baryonic TF-like relation for the sample of galaxies using  $(M/L)_{\text{epc}}^R = 1.0$ . Mass or associated luminosity is given as a function of velocity at the observed, flat outer part of the rotation curve. There is an exquisite linear relation over a mass range spanning more than  $2\frac{1}{2}$  orders of magnitude. The fit of a straight line gives a slope of  $3.7 \pm 0.2$  (dashed). In addition a more classic TF relation, with no population correction and no gas mass included, is given by displacing the data points to the ends of the attached solid lines.

both directions into account (Reed 1989) giving a slope of  $3.7 \pm 0.2$  and reduced  $\chi^2$  of 2.5.

A second TF-like relation is given in Fig. 13 where the total baryonic mass has been plotted versus the maximum rotation of the pseudo isothermal halo resulting from the direct (non A-de-C) fit to the individual rotation curves. Again there is a good linear relation with a slope of  $4.3 \pm 0.4$  and reduced  $\chi^2$  of 4.8 thus being slightly steeper than that of the previous TF-like relation. This is explained easily by the fact that for the least luminous galaxies the fitted halo rotation curve continues to rise beyond the last measured rotational points. The asymptotic halo maximum rotation is then relatively larger compared to that of the more massive galaxies. As is obvious, the scatter for this relation (Fig. 13) is larger compared with that of the previous one in Fig. 12. This may be explained by the inclusion of the rotational effect of the baryonic component into the observed value of  $v_{\text{flat}}$  on the x-axis of Fig. 12. That creates a moderate correlation between the ordinate and abscissa making the scatter smaller compared to that of the completely uncorrelated axes in Fig. 13. In both TF-like relations NGC 3198 is slightly deviating in the sense that it is too massive (or bright) for its rotation. This is likely caused by the fact that NGC 3198 contains a large amount of gas compared to its light (see Table 1) such that for this galaxy more mass in the form of gas has fallen into its halo.

The original Tully-Fisher relation (Tully & Fisher 1977) is a relation between the absolute magnitude of a galaxy, corrected for extinction, and the line width of the H I profile, corrected for inclination and internal broadening. Depend-

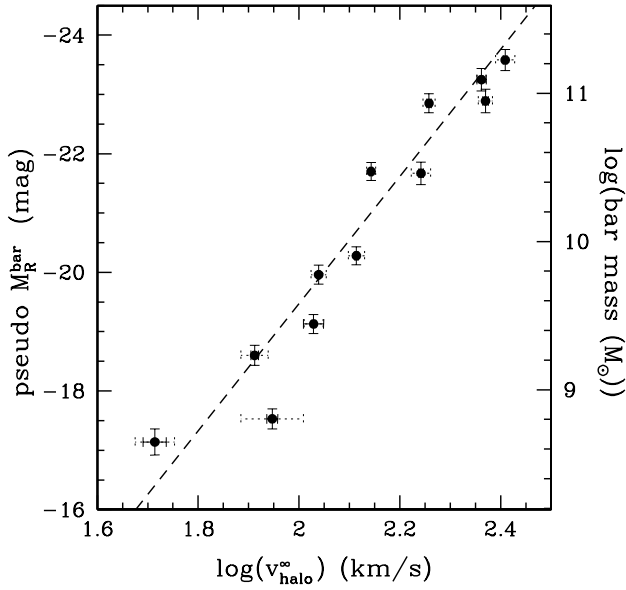


**Figure 13.** As Fig. 12, but now baryonic mass is plotted versus the maximum rotation of a pseudo isothermal dark halo resulting from the fit to the observed rotation curves as in Fig. 9. Errorbars in the x-direction give the formal error by the drawn lines and the error estimate by eye, equal to that in Fig. 12, by the dashed lines. A fit of a straight line to the data (dashed line) has a slope of  $4.3 \pm 0.4$ .

ing on the way the observations are being treated and the way the corrections are applied, generally a different relation is found. The two relations presented here, in a natural way, contain much less intricacies compared to the classical relation. At first, the rotation is used instead of the line width. Furthermore, a population correction is applied to the luminous component and gas mass is added to obtain a total baryonic mass. This should automatically remove two deviating features or specific “kinks” associated with the classical TF relation (see Noordermeer & Verheijen 2007). Usually the brightest galaxies appear to be somewhat too faint for their rotation. This kink at the bright end can be largely removed by taking the rotations at the flat asymptotic part of the rotation curve and by using near infra-red colours instead of optical colour to diminish absorption and population effects. A second deviation at the faint end, below  $v_{\text{rot}} \sim 90 \text{ km s}^{-1}$ , exists. This kink can be eliminated by using the baryonic TF relation (McGaugh et al. 2000) thus including the gas mass which generally constitutes a larger fraction for the fainter spiral galaxies.

To investigate these matters for the present sample, also a more classic TF relation has been put together. No population correction is applied, only the extinction corrections, which for the systems with bulges have been applied to the total light using the inclinations derived from the H I velocity field. The maximum observed rotation is taken and gas mass has not been included. Then a correlation between the R-band luminosity and rotation is constructed and is displayed in Fig. 12 by a displacement of the datapoints. Instead of a linear relation a curved relation is present as expected following the discussion in the preceding paragraph.

In general, the main conclusion of studies dealing with

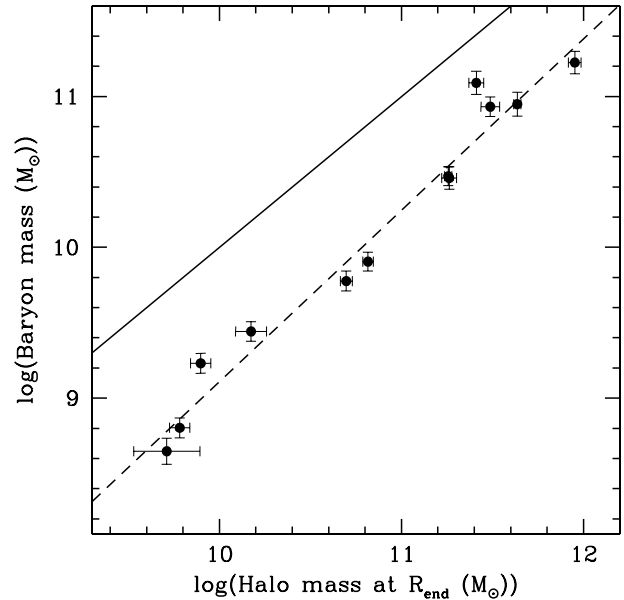


**Figure 14.** The baryonic mass of the galaxies using the universal  $(M/L)_{\text{epc}}^R = 1.0$ , as a function of total mass of the dark halo at the radius of the outermost measured rotation. The apparent well established correlation confirms the notion that there is a fundamental relation between the mass of the dark halo and the mass of the baryons that have fallen in. The full drawn line represents unity; the dashed line is a linear fit to the data, having a slope of  $1.14 \pm 0.07$ . It appears that more massive galaxies contain a larger fraction of baryons; typically the ratio of DM to baryons is  $\sim 9$  for small galaxies and  $\sim 5$  for large galaxies. (Mind: data points of NGC 3198 and NGC 2903 nearly coincide).

TF relations is that there must be a fundamental relation between the mass of the dark halo and the mass of the baryons that have fallen in. For the present study the same conclusion may be drawn based on the tight linear relations that have been derived and are presented in Figs 12 and 13. Yet for the assumed universal M/L ratio and ensuing dark halo properties that conclusion can be checked more directly. The total baryonic mass is known for each galaxy. In addition the rotation curves of the adiabatically de-contracted halos, which represent the pre formation halo structures, are given in Fig. 10. From that the cumulative mass of these halos until the last measured data point can be calculated directly, which has been done actually. In a number of cases, however, the outermost rotational points of the halos show some scatter. Therefore, to obtain a representative value for the velocity at the end of the measurements (at  $R_{\text{end}}$ ) the rotation at the end of the fit of the pseudo isothermal rotation curve to the data points is taken. The error on this value is estimated by eye. Then in Fig. 14 the baryonic mass is plotted versus the halo mass at  $R_{\text{end}}$ . As can be seen, indeed, there is a clear and rather linear relation between the two mass parameters, now confirming directly the main suggestion of TF studies. Inspection of Fig. 14 shows that it appears that the more luminous galaxies contain a relatively larger fraction of baryons. But, there is a caveat, however. Not the total halo mass is presented but only the mass until the outermost measured rotational point. So only conclusions can be drawn concerning masses until that radius.

## 10 DISCUSSION AND CONCLUSIONS

Some general matters will be addressed and some items will be discussed in more detail. Finally the main conclusions are given point by point.

### 10.1 Comparing the four fitting procedures

Four fitting procedures have been employed, in principle each with two free parameters. Comparing these four can be done by inspecting figures 2, 4, 7, and 9, and judging the quality of the fits. All fits have been achieved by minimizing the  $\chi^2$  difference between model and data, but as discussed in Sect. 4, care has to be taken when interpreting this minimum value of  $\chi^2$ . An inspection by eye may yield additional and a more general insight.

One can immediately notice that the NFW fit is by far the worst, certainly for the least luminous galaxies. In that case for the other galaxies the contribution of the luminous component is forced to low values. An NFW halo is simply too concentrated to be able to properly represent the dark matter in a galaxy. For the other three procedures, the quality of the fits is comparable. MOND-like generally converges to a maximum disc contribution for the massive galaxies, but to a submaximum disc situation for the least massive systems. That procedure has also a slight problem fitting the rotation curves for NGC 5585 and NGC 3109. As noted in sections 5 and 6, a maximum disc contribution leads to a M/L ratio, corrected for extinction and population effects, which varies considerably from galaxy to galaxy with a general trend to decrease with a factor of two going from the least to the most massive systems. Such a change in M/L ratio is not to be favoured, or at least it is difficult to explain.

It appears that the MOND-like fitting procedure generates a considerable range of values for the free parameter  $a_0$ , and thus, like the maximum disc or equal M/L procedure also two free parameters are required to make the fits. One may wonder if there is a fundamental difference between MOND-like and the other two. To assess this matter, it should be considered what the fitting does in each case. MOND-like as it has been applied here, keeping the distances fixed, uses Eq. (8) to scale up the Newtonian rotation. Instead the other fitting schemes add the rotation of supposed dark matter to the Newtonian rotation. As such, all use a two parameter scaling of the already existing rotation of the luminous matter. Yet, for MOND-like the scaling parameters are both in the direction of the velocity, while for fixed M/L values with a dark halo, one parameter scales in the velocity and the other in the radial direction. So there is a fundamental difference and the adding of dark matter is a more flexible method. But by no means, judging the fits of the present sample, one method is to be preferred over the other.

The maximum disc procedure maximizes the amount of luminous matter and minimizes the amount of dark matter. Hence the result is certainly useful in constraining properties of galaxies. In the paper by Van Albada & Sancisi (1986) discussing the maximum disc principle a number of arguments are presented favouring a maximum baryonic contribution. However none of these arguments present any hard evidence. Observations of stellar velocity dispersions (Bottema 1993;

Kregel et al. 2005) lead to a sub maximum contribution, yet, locally in the disc the baryonic matter dominates. This observation in combination with the adoption of a universal M/L ratio, provides the fitting scheme described in Sect. 9 and in Fig. 9. The results of this scheme are by no means worse than those of the maximum disc or MOND-like fits, and in some cases even better. So being physically and observationally motivated, and providing a good representation of the observed rotations, that procedure is preferred. Because of that a rather extensive analysis is made of the predicted dark matter properties following from the universal M/L ratio method. Results from that analysis should be useful in constraining dark halo and galaxy formation scenarios.

### 10.2 H I scaling

It appears that for spiral galaxies, the ratio of total mass to H I mass in the outer regions is roughly constant (Bosma 1981; Carignan & Beaulieu 1989; Broeils 1992a, b). As a consequence it might be argued that the observed extended flat rotation curves can be explained by scaling up the gas rotational contribution, a procedure called H I scaling. These matters have been investigated in some detail by Hoekstra et al. (2001), who showed that this procedure works well to explain the observed shapes of the rotation curves for a sample of 24 spiral galaxies of various morphological types. They found an average H I scaling factor of 9; correcting for the presence of helium, this implies a total gas scaling factor of approximately 6.5. Hoekstra et al. found a systematic trend with luminosity, lower luminosity galaxies require a lower gas scaling factor and vice versa. Later on these matters have been addressed by Swaters (1999) for a sample of dwarf spiral galaxies and by Noordermeer (2006) for a sample of early type spirals. It appears that the dwarfs require substantially smaller scaling factors than Hoekstra et al. found and that the early types, in many cases, require substantially larger scale factors.

For the sample in this paper the H I scaling has also been investigated. The results were rather disappointing. In three cases the fit is bad in all respects. For the rest, generally, the global correspondence between fit and data is reasonable, however in most cases there is a misfit for details. There are two cases (NGC 2998 and NGC 6503) where the global fit is good and the detailed fit reasonable, while only one case (NGC 3198) gives an excellent fit. The total gas scale factor shows a considerable range, from 4.7 to 22.5, seven galaxies have values around 6.5, but five out of 12 have substantially larger values. Considering the discussion and findings above, it is obvious that there is not a universal gas scaling factor. The rotation curve fit then needs two parameters: M/L ratio and gas scale, and as such does not improve on other fit procedures.

### 10.3 Accuracy of the M/L ratios

The uncertainties of the employed M/L ratios stem from a couple of sources. At first the distance errors. For those determined by the Cepheid method the error is typically  $\lesssim 10\%$ ; the distances of the other galaxies are less certain. M/L scales inversely linear with distance and so the error is passed on linearly.

Concerning the determination of the total amount of light one is hampered by the uncertainties of the extinction and population corrections. For the extinction corrections, a well motivated and well supported method is used; dependent on the total luminosity of a galaxy, as should be done for a sample with a large range of masses (Tully et al. 1998). The internal absorption correction of a face-on galaxy is less certain, but this correction is always relatively small and consequently the error of the method is of less influence. A reasonable estimate of the total extinction error is 0.12 magnitudes.

The population correction as such is rather well determined. Bell & de Jong (2001) have extensively tested the M/L dependence on colour for several galaxy formation scenarios and for several population synthesis codes. In all cases a tight correlation is found for the optical passbands. Going to the near infra-red, M/L becomes dependent on metallicity and age too. Consequently for a sample with broad galaxy parameters near infra-red colours should be avoided when restricting M/L ratios. At present, the main error stems from the uncertainty of the absorption corrected B-V colour. It is practically impossible to derive this correction on B-V from basic principles for a patchy dust distribution in combination with local star formation activity for a spiral galaxy. Instead the empirical procedure of the RC3 is used which is estimated to give, on average, an error of  $\sim 15\%$  on the population correction. Adding the errors for distance, extinction, and population correction in quadrature one ends up at a total error slightly larger than 20%. That implies approximately an error of 10% for rotational velocities; though it has to be kept in mind that for galaxies with uncertain distances this error can be significantly larger.

#### 10.4 Where do the dark halos end?

In this paper it is demonstrated that the pseudo isothermal density functionality gives an excellent description of the density distribution of dark halos. But, as can readily be noticed, the  $R^{-2}$  functionality at large radii generates a mass which increases linearly with  $R$ . At some point the halo has to end; meaning that the density at some point has to deviate from pseudo isothermal.

As discussed in Sect. 9, for a fair number of galaxies a density law according to Burkert (1995) is not in agreement with the determined rotation of the dark halo. A Burkert halo has an isothermal centre in combination with an  $R^{-3}$  decrease at large radii. Obviously such a density functionality drops off too quickly and in reality a density  $\propto R^{-2}$  over an extended range is necessary. This conclusion agrees with the same finding from an analysis of strong lensing observations for early type galaxies (Koopmans et al. 2006).

Is there a sudden end to the dark halo or a smooth transition to the ambient density of the local universe? The former possibility seems to be suggested by the galaxy DDO 154. For that system, dominated by gas, the observed rotation drops nearly Keplerian beyond a radius of 5.5 kpc ( $\sim 11h$ ), which indicates a sudden end of the dark halo. However, such a drop is only observed for one case. As such the evidence is not overwhelming. Moreover, because the galaxy is not massive, the rotation is small, and the velocity field is poorly resolved. A confirmation of this drop is needed

and more HI rich dwarf galaxies might be investigated for the presence of this phenomenon.

#### 10.5 Cores generated by SIDM?

The analysis of this paper adds to the evidence that the central regions of DM halos have a central constant density core. This contradicts the result of halo formation calculations using collisionless DM which inevitable, by violent relaxation, produces a central cusp with a density proportional to  $R^{-0.5 \rightarrow -1.5}$  (NFW, Moore et al. 1999, Diemand et al. 2004). To solve this contradiction one can invoke astrophysical processes to save CDM (see the introduction for a discussion), or alternatively explore other kinds of DM (Davé et al. 2001, and references therein). Anyway, looking at the available evidence to date, the constant density core emerges triumphantly everywhere. An obvious and well known astrophysical counterpart of such a structure is a globular cluster. The formation of these is supposed to have taken place by the collapse of giant gas clouds, primarily in the early universe. By solving the spherically symmetric, virialized gravothermal fluid equations (Lynden-Bell & Eggleton 1980) the formation and structure of globular clusters can be explained. By the similarity of cored halos and globulars one is then drawn to the suggestion that halos may also have been formed by gas-like of self interactive processes.

Such an idea of Self Interacting DM (SIDM) has been investigated semi analytically (Spergel & Steinhardt 2000; Ahn & Shapiro 2005) and numerically (Yoshida et al. 2000; Davé et al. 2001; Colín et al. 2002). Obviously the problem is more complicated than that of a collisionless situation and results to date are rather preliminary. One clear and non controversial finding is that SIDM can indeed produce halos with cores, for an intermediate range of realistic DM particle scattering cross sections. In a cosmological setting these cores can be stable over a Hubble time. Controversy exists over whether the size of the cores varies with mass of the halo or with cosmological environment. It appears that SIDM generates cores with equal central densities because this density is essentially set by collisional physics. These densities are comparable to the observed densities of halos of LSB and/or dwarf galaxies (Firmani et al. 2001), ranging between 0.01 to 0.04  $M_{\odot} \text{pc}^{-3}$ .

At this stage a comparison can be made of the SIDM predictions with the result of the rotation curve decompositions, especially those of Sect. 9 for a universal M/L ratio. The core radii of the dark halos derived from the decompositions appear to be rather independent of galaxy and halo mass (Fig. 11), if any, the core radii of the smallest and most LSB galaxies are a factor of two larger than those of the intermediate and larger sized galaxies. The simulations of Davé et al. and Colín et al. seem to indicate that more massive halos have larger core radii, although the resolutions are still poor and results preliminary. Central halo densities of the four smallest galaxies are in the range of 0.01 to 0.03  $M_{\odot} \text{pc}^{-3}$ , in agreement with the findings of Firmani et al. and with the numerical SIDM calculations. For the intermediate galaxies without bulges, however, the central halo density is found to be a factor of ten larger. This contradicts the SIDM results at first sight. On the other hand, the galaxies investigated here are rather isolated and cores

made up of self interacting particles might have undergone various stages of collapse, because they lack heat input by continual infall of DM. In this respect it is interesting to note that the galaxies with bulges seem to have a lower central core density again. Hypothetically that could suggest a kind of bulge-DM interaction or replacement during the initial stages of galaxy formation. Anyway, the derived structure of dark halos from the present analysis of a sample of galaxies with a broad range of sizes and properties, can set clear limitations to any possible alternative to collisionless DM.

## 10.6 Conclusions

(i) For a maximum disc situation with a pseudo isothermal dark halo excellent fits can be made to the observed rotation curves. Yet an uncomfortably large range of M/L ratios is required.

(ii) A MOND fitting scheme with the two free parameters,  $a_0$  and mass-to-light ratio, can give a good representation of the observed rotations.

(iii) MOND with only one free parameter, the M/L ratio of the luminous component, cannot explain the rotation curves for all galaxies simultaneously, not even when the distances to the galaxies are stretched to their limits.

(iv) In case of an adopted NFW dark halo the rotation curves of the 8 most massive galaxies can be explained well, but in some cases only for unrealistically small M/L ratios.

(v) For the four least luminous galaxies an NFW halo is clearly inconsistent with the observations.

(vi) The central regions of galaxies definitively have cores and not cusps.

(vii) When adopting a universal M/L ratio for all galaxies, corrected for extinction and populations effects, the rotational contribution of the luminous components becomes fixed a priori.

(viii) For that assumption, in combination with a pseudo isothermal dark halo, excellent fits to the observed rotation curves can be made.

(ix) At the mean time, the rotational contribution of the disc is then sub maximal being in agreement with the observed stellar velocity dispersions.

(x) The core radii of the resultant halos are typically one to a few kpc, apparently independent of galaxy mass.

(xi) Such a universal M/L ratio generates very linear baryonic TF relations.

(xii) In addition a ratio between dark and baryonic mass is then determined which ranges between  $\sim 9$  for small galaxies and  $\sim 5$  for large galaxies, at the outermost measured rotation.

## REFERENCES

- Ahn, K., & Shapiro, P.R. 2005, MNRAS, 363, 1092  
 Begeman, K. 1987, PhD Thesis, University of Groningen  
 Begeman, K. 1989, A&A 223, 47  
 Begeman, K.G., Broeils, A.H., & Sanders, R.H. 1991, MNRAS, 249, 523 (BBS)  
 Bekenstein, J.D. 2004, Phys. Rev. D 70, 083509  
 Bell, E. F., & de Jong, R. S. 2001, ApJ 550, 212  
 Blais-Ouellette, S., Carignan, C., Amram, P., & Côté, S. 1999, AJ 118, 2123  
 Blais-Ouellette, S., Amram, P., & Carignan, C. 2001, AJ 121, 1952  
 Blais-Ouellette, S., Amram, P., Carignan, C., & Swaters, R. 2004, A&A, 420, 147  
 Blumenthal, G. R., Faber, S. M., Flores, R., & Primack, J. R. 1986, ApJ, 301, 27  
 Bond, J.R., Kofman, L., Pogosyan, D. 1996, Nature 380, 603  
 Bosma, A. 1978, PhD Thesis, University of Groningen  
 Bosma, A. 1981, AJ, 86, 1791  
 Bottema, R. 1988, A&A, 197, 105  
 Bottema, R. 1989, A&A, 221, 236  
 Bottema, R. 1993, A&A, 275, 16  
 Bottema, R. 1997, A&A, 328, 517  
 Bottema, R. 1999, A&A, 348, 77  
 Bottema, R. 2002, A&A, 388, 809  
 Bottema, R. 2003, MNRAS, 344, 358  
 Bottema, R., & Kregel, M. 2014, in preparation  
 Bottema, R., & Verheijen, M. A. W. 2002, A&A 388, 793  
 Bottema, R., Pestaña, J.L.G., Rothberg, B., & Sanders, R.H. 2002, A&A 393, 453 (BPRS)  
 Broeils, A.H. 1992a, PhD. Thesis, University of Groningen  
 Broeils, A.H. 1992b, A&A, 256, 19  
 Bullock, J.S., Kolatt, T.S., Sigad, Y., et al. 2001, MNRAS, 321, 559  
 Burkert, A. 1995, ApJ, 447, L25  
 Carignan, C., & Beaulieu, S. 1989, ApJ 347, 760  
 Carignan, C., & Freeman, K.C. 1988, ApJ, 332, L33  
 Carignan, C., & Purton, C. 1998, ApJ 506, 125 (CP98)  
 Casertano, S. 1983, MNRAS, 203, 735  
 Casertano, S., & van Gorkom, J.H. 1991, AJ 101, 1231  
 Choi, J.-H., Lu, Y., Mo, H. J., & Weinberg, M. D. 2006, MNRAS, 372, 1869  
 Colín, P., Avila-Reese, V., Valenzuela, O., & Firmani, C. 2002, ApJ, 581, 777  
 Côté, S., Carignan, C., & Sancisi, R. 1991, AJ 102, 904  
 Courteau, S., & Rix, H.W. 1999, ApJ 513, 561  
 Davé, R., Spergel, D.N., Steinhardt, P.J., & Wandelt, B.D. 2001, ApJ, 547, 574  
 Davis, M., Efstathiou, G., Frenk, C.S., White, S.D.M. 1985, ApJ 292, 371  
 de Blok, W. J. G., & Bosma, A. 2002, A&A 385, 816  
 de Blok, W.J.G., & McGaugh, S.S. 1998, ApJ 508, 132  
 de Blok, W.J.G., McGaugh, S.S., Bosma, A., & Rubin, V.C. 2001a, ApJ, 552, L23  
 de Blok, W.J.G., McGaugh, S.S., & Rubin, V.C. 2001b, AJ, 122, 2396  
 de Blok, W.J.G., Bosma, A., & McGaugh, S.S. 2003, MNRAS 340, 657  
 de Blok, W.J.G., Walter, F., Brinks, E., et al. 2008, AJ, 136, 2648  
 de Jong, R.S. 1996, A&AS, 118, 557  
 de Vaucouleurs, G., de Vaucouleurs, A., Corwin, H.G., et al. 1991, Third Reference Catalogue of Bright Galaxies (Springer verlag, New York), (RC3)  
 Diemand, J., Moore, B., & Stadel, J. 2004, MNRAS, 353, 624  
 Drozdovsky, I. O., & Karachentsev, I. D. 2000, A&AS 142, 425  
 Dutton, A.A., Courteau, S., de Jong, R.S., & Carignan, C. 2005, ApJ 619, 218  
 Firmani, C., D'Onghia, E., Chincarini, G., Hernández, X., & Avila-Reese, V. 2001, MNRAS, 321, 713  
 Freedman, W. L., & Madore, B. F. 1988, ApJ 332, L63  
 Freedman, W. L., Madore, B. F., Gibson, B. K., et al. 2001, ApJ, 553, 47  
 Garrison-Kimmel, S., Rocha, M., Boylan-Kolchin, M. & al. 2013, MNRAS, 433, 3539  
 Gentile, G., Famaey B. & de Blok, W.J.G. 2010, A&A, 527, A76+  
 Gentile, G., Salucci, P., Klein, U., Vergani, D., & Kalberla, P. 2004, MNRAS 351, 903

- Gnedin, O. Y., Kravtsov, A. V., Klypin, A. A., & Nagai, D. 2004, *ApJ*, 616, 16
- Governato, F., Brook, C., Mayer, L., et al. 2010, *Nature*, 463, 203
- Herrmann, K.A. & Ciardullo, R. 2009, *ApJ*, 705, 1686
- Hernquist, L. 1990, *ApJ*, 356, 359
- Hoekstra, H., van Albada, T.S., & Sancisi, R. 2001, *MNRAS*, 323, 453
- Hughes, S. M. G., Han, M., Hoessel, J., et al. 1998, *ApJ*, 501, 32
- Jesseit, R., Naab, T., & Burkert, A. 2002, *ApJ*, 571, L89
- Jing, Y.P. 2000, *ApJ*, 535, 30
- Jobin, M., & Carignan, C. 1990, *AJ* 100, 648
- Karachentsev, I. D., & Sharina, M. E. 1997, *A&A* 324, 457
- Kelson, D. D., Illingworth, G. D., Saha, A., et al. 1999, *ApJ*, 514, 614
- Kennicutt, R.C. Jr., Armus, L., Bendo, G, et al. 2003, *PASP*, 115, 928
- Kent, S.M. 1986, *AJ*, 91, 1301 (K86)
- Kent, S.M. 1987, *AJ*, 93, 816 (K87)
- Knapp, G., & Kormendy, J. (eds) 1987, in *IAU Symp. No. 117, Dark matter in the universe* (Reidel Pub. Dordrecht)
- Koopmans, L.V.E., Treu, T., Bolton, A.S., Burles, S., Moustakas, L.A. 2006, *ApJ* 649, 599
- Kregel, M., van der Kruit, P.C., & Freeman, K.C. 2005, *MNRAS* 358, 503
- Krismmer, M., Tully, R. B., Gioia, I. M. 1995, *AJ* 110, 1584
- Kroupa, P. 2001, *MNRAS*, 322, 231
- Lake, G. 1989, *ApJ*, 345, L17
- Lauberts, A., & Valentijn, E. A. 1989, *The Surface Photometry Catalogue of the ESO- Uppsala Galaxies*, (European Southern Observatory, Garching), p. 10
- Lee, M. G., & Madore, B. F. 1993, *AJ* 106, 964
- Longo, G., & de Vaucouleurs, A. 1994, *A General Catalogue of Photoelectric Magnitudes and Colors in the U, B, V system of 3578 Galaxies Brighter than the 16th Magnitude*, University of Texas Monographs in Astronomy, No. 3
- Ludlow, A.D., Navarro, J.F., Angulo, R.E., et al. 2014, *MNRAS*, 441, 378
- Lynden-Bell, D., & Eggleton, P.P. 1980, *MNRAS*, 191, 483
- Macciò, A.V., Dutton, A.A., van den Bosch, F.C., et al. 2007, *MNRAS*, 378, 55
- Macciò, A.V., Dutton, A.A. & van den Bosch, F.C. 2008, *MNRAS*, 391, 1940
- Macri, L. M., Stetson, P. B., Bothun, G. D., Freedman, W. L., Garnavich, P. M., Jha, S. Madore, B. F., & Richmond, M. W. 2001, *ApJ*, 559, 243
- Marcelin, M., Boulesteix, J., & Georgelin, Y. 1983, *A&A* 128, 140
- Martinsson, T.P.K., Verheijen, M.A.W., Westfall, K.B., et al. 2013, *A&A*, 557, A131
- McGaugh, S. S., & de Blok, W. J. G. 1998, *ApJ*, 499, 66
- McGaugh, S.S., Schombert, J.M., Bothun, G.D., & de Blok, W.J.G. 2000, *ApJ*, 533, L99
- Milgrom, M. 1983 *ApJ*, 270, 365
- Milgrom, M. 1988, *ApJ*, 333, 689
- Moore, B., Quinn, T., Governato, F., Stadel, J., & Lake, G. 1999, *MNRAS*, 310, 1147
- Musella, I., Piotto, G., & Capaccioli, M. 1997, *AJ* 114, 976
- Navarro, J.F. 1998, [*astro-ph/9807084*]
- Navarro, J.F., Frenk, C.S., & White, S.D.M. 1997, *ApJ*, 490, 493 (NFW)
- Neto, A.F., Liang, G., Bett, P.B., et al. 2007, *MNRAS*, 381, 1450
- Noordermeer, E. 2006, *PhD. Thesis*, University of Groningen
- Noordermeer, E., & Verheijen, M. A. W. 2007, *MNRAS*, 381, 1463
- Peñarrubia, J., Pontzen, A., Walker, M.G. & al. 2012, *ApJ*, 759, L42
- Persic, M., Salucci, P. & Stel, F. 1996, *MNRAS*, 281, 27
- Pontzen, A. & Governato, F. 2012, *MNRAS*, 421, 3464
- Prada, F., Gutierrez, C. M., Peletier, R. F., & McKeith, C. D. 1996, *ApJ*, 463, L9
- Randriamampandry, T. & Carignan, C. 2014, *MNRAS*, 439, 2132
- Read, J.I. & Gilmore, G. 2005, *MNRAS*, 356, 107
- Reed, B.C. 1989, *Am. J. Phys.*, 57 (7), 642
- Rubin, V. C., Burbidge, E. M., Burbidge, G. R., Crampin, D. J., & Prendergast, K. H. 1965, *ApJ*, 141, 759
- Rubin, V. C., Burstein, D., Ford, W. K., Jr., & Thonnard, N. 1985, *ApJ*, 289, 81
- Salpeter, E.E. 1955, *ApJ* 121, 161
- Salucci, P., Walter, F., & Borriello, A. 2003, *A&A*, 409, 53
- Sancisi, R., & van Albada, T.S. 1987, in *IAU Symp. 117, Dark matter in the universe*, ed. J. Kormendy, & G. Knapp (Reidel Pub. Dordrecht), 67
- Sanders, R.H. 1990, *A&A Rev.*, 2, 1
- Sanders, R. H. 1996, *ApJ*, 473, 117
- Sanders, R. H., & McGaugh S. S. 2002, *ARA&A*, 40, 263
- Sanders, R. H., & Verheijen, M. A. W. 1998, *ApJ*, 503, 97
- Schlegel, D. J., Finkbeiner, D. P., & Davis, M. 1998, *ApJ* 500, 525
- Silk, J. 1987, in *A Unified View of the Macro- and Micro-Cosmos*, eds. A. de Rujula, D.V. Nanopoulos, P.A. Shaver (World Scientific, Singapore), p. 277
- Simon, J.D., Bolatto, A.D., Leroy, A., & Blitz, L. 2003, *ApJ* 596, 957
- Soszyński, I., Gieren, W., Pietrzyński, G., Bresolin, F., Kudritzki, R.-P., & Storm, J. 2006, *ApJ*, 648, 375
- Spergel D.N., Bean, R., Doré, M.R., et al. 2007, *ApJS*, 170, 377
- Spergel, D.N., & Steinhardt, P.J. 2000, *Phys. Rev. Lett.*, 84, 3760
- Swaters, R.A. 1999, *PhD. Thesis*, University of Groningen
- Swaters, R.A., & Balcells, M. 2002, *A&A* 390, 863
- Swaters, R.A., Sanders, R.H. & McGaugh, S.S. 2010, *ApJ*, 718, 380
- Thuan, T.X., & Gunn, J.E. 1976, *PASP* 88, 543
- Trimble, V. 1987, *ARA&A* 25, 425
- Tully, R. B., & Fisher, J. R. 1977, *A&A* 54, 661
- Tully, R. B., & Fouqué, P. 1985, *ApJS* 58, 67
- Tully, R. B., & Pierce, M. J. 2000, *ApJ* 533, 744
- Tully, R. B., Verheijen, M. A. W., Pierce, M. J., Huang, J.-S., & Wainscoat, R. J. 1996, *AJ*, 112, 2471
- Tully, R. B., Pierce, M. J., Huang, J.-S., Saunders, W., Verheijen, M. A. W., & Witchalls, P. L. 1998, *AJ*, 115, 2264
- van Albada, T.S., & Sancisi, R. 1986, *Phil. Trans. R. Soc. London, Ser. A* 320, 447
- van Albada, T. S., Bahcall, J. N., Begeman, K., & Sancisi, R. 1985, *ApJ*, 295, 305
- van der Kruit, P.C., & Searle, L. 1981, *A&A*, 95, 105
- van der Kruit, P.C., & Searle, L. 1982, *A&A*, 110, 61
- Verheijen, M. A. W. 2001, *ApJ*, 563, 694
- Wevers, B. M. H. R., van der Kruit, P. C., & Allen, R. J. 1986, *A &AS*, 66, 505
- Yoshida, N., Springel, V., White, S.D.M., & Tormen, G. 2000, *ApJ*, 535, L103

## APPENDIX A: TABLES

This paper has been typeset from a  $\text{\TeX}$ / $\text{\LaTeX}$  file prepared by the author.

**Table A1.** Properties of whole galaxies

Galaxy	Profile in band	Opt. incl. of disc ( $^{\circ}$ ) ( $q_0 = 0.11$ )	H I kin. incl. ( $^{\circ}$ )	Dist. (Mpc)	$L_{\text{tot}}$ observed ( $10^9 L_{\odot}^R$ )	b/d ratio	Gas mass ( $10^9 M_{\odot}$ )	$M_{\text{gas}}/L_{\text{tot}}^R$
N2841	r	66	68	14.1	40.74	0.53	28.4	0.70
N3992	I	57	57	18.6	32.44	0.29	8.53	0.26
N7331	I	?	75	14.72	31.15	1.11	15.8	0.51
N2998	r	61	58	67.4	37.8	0	30.5	0.81
N2903	r	62	62	7.6	14.4	0	4.41	0.31
N3198	r	66	71	13.8	11.48	0	15.5	1.35
N2403	r	50	60	3.22	4.69	0	4.09	0.87
N6503	R	74	74	5.2	2.36	0	1.84	0.78
N5585	R	52	52	6.2	1.12	0	1.82	1.63
N1560	R	82	80	3.1	0.26	0	1.22	4.82
N3109	I	75	70	1.36	0.19	0	0.45	2.43
D154	R	56	64	3.8	0.029	0	0.43	15.1

**Table A2.** Luminosities and extinction corrections in the R-band

Galaxy	$L_{\text{tot}}^{\text{obs}}$ uncor. ( $10^9 L_{\odot}^R$ )	Abs. Lum. uncor. (mag.)	$\frac{a}{b}$	$A^b$ (mag.)	$A^{i=0}$ (mag.)	$A^{i=0}$ (mag.)	Abs. Lum. corrected (mag.)	$L_{\text{ec}}^{\text{tot}}$ ext. corr. ( $10^9 L_{\odot}^R$ )
N2841b	14.11	-20.89	1	0.042	0.2*	0	-21.13	17.57
N2841d	26.63	-21.58	2.58	0.042	0.61	0.26	-22.49	61.60
N3992b	7.29	-20.18	1	0.078	0.2*	0	-20.46	9.44
N3992d	25.15	-21.52	1.79	0.078	0.358	0.25	-22.21	47.25
N7331b	16.39	-21.06	1	0.242	0.2*	0	-21.50	24.71
N7331d	14.76	-20.94	3.57	0.242	0.783	0.25	-22.22	47.64
N2998	37.8	-21.96	2.04	0.035	0.477	0.27	-22.74	77.26
N2903	14.4	-20.92	2.08	0.083	0.409	0.23	-21.64	28.05
N3198	11.48	-20.67	2.5	0.034	0.490	0.22	-21.41	22.70
N2403	4.69	-19.70	1.54	0.107	0.177	0.17	-20.15	7.11
N6503	2.36	-18.95	3.63	0.085	0.462	0.15	-19.65	4.49
N5585	1.12	-18.14	1.61	0.042	0.111	0.10	-18.39	1.41
N1560	0.26	-16.54	4.74	0.504	0.191	0.05	-17.29	0.51
N3109	0.19	-16.19	3.57	0.178	0.047	0.02	-16.44	0.23
D154	0.029	-14.16	1.75	0.025	0	0	-14.19	0.029

\*: estimated

**Table A3.** Population corrections in the R-band

Galaxy	$(B - V)_0^T$ (RC3)	M/L acc. to (B&deJ)	M/L scaled to $(B - V) = 0.6$	$L_{\text{epc}}^{\text{tot}}$ ( $10^9 L_{\odot}^R$ )
N2814b	1.05	4.20	3.55	62.30
N2841d	0.68	1.48	1.25	77.12
N3992b	0.94	3.08	2.60	24.56
N3992d	0.66	1.40	1.18	55.90
N7331b	1.0	3.65	3.08	76.13
N7331d	0.45	0.78	0.66	31.20
N2998	0.48	0.84	0.71	55.09
N2903	0.55	1.03	0.87	24.35
N3198	0.43	0.73	0.62	14.07
N2403	0.39	0.66	0.55	3.94
N6503	0.57	1.09	0.92	4.13
N5585	0.46	0.80	0.67	0.95
N1560	0.57	1.09	0.92	0.47
N3109	0.52	0.95	0.80	0.19
D154	0.32	0.54	0.45	0.013

**Table A4.** Maximum disc fits

Galaxy	$(M/L)_{\text{obs}}$ $(M_{\odot}/L_{\odot}^R)$	$(M/L)_{\text{epc}}$ $(M_{\odot}/L_{\odot}^R)$	$v_{\text{max}}^h$ (km s <sup>-1</sup> )	Err. (km s <sup>-1</sup> )	$R_{\text{core}}^h$ (kpc)	Err. (kpc)
N2841b	5.67	1.28				
N2841d	6.04	2.09	292.9	7.6	13.9	1.3
N3992b	6.48	1.92				
N3992d	5.35	2.41	326.9	15.1	23.2	1.8
N7331b	4.31	0.93				
N7331d	3.23	1.53	253.0	6.8	11.0	0.8
N2998	4.36	2.99	254.9	55.4	32.5	10.9
N2903	3.79	2.24	175.8	3.4	4.92	0.31
N3198	3.96	3.23	153.1	2.9	11.23	0.64
N2403	3.00	3.57	151.8	3.9	6.21	0.40
N6503	4.37	2.50	124.7	2.1	4.33	0.22
N5585	1.16	1.37	115.5	6.4	3.61	0.39
N1560	5.44	2.96	135.8	9.4	7.95	0.73
N3109	3.06	3.04	116.0	7.3	5.17	0.47
D154	4.26	9.21	59.1	3.8	2.03	0.11

**Table A5.** MOND fits

Galaxy	$(M/L)_{\text{obs}}$ $(M_{\odot}/L_{\odot}^R)$	$(M/L)_{\text{epc}}$ $(M_{\odot}/L_{\odot}^R)$	Err.	$a_0$ (10 <sup>-8</sup> cm s <sup>-2</sup> )	Err. (10 <sup>-8</sup> cm s <sup>-2</sup> )
N2841b	5.67	1.28	0.13		
N2841d	6.17	2.13	0.17	1.55	0.06
N3992b	7.20	2.14	0.21		
N3992d	4.34	1.95	0.15	1.43	0.10
N7331b	4.49	0.97	0.07		
N7331d	2.93	1.39	0.20	1.51	0.05
N2998	4.08	2.80	0.16	0.53	0.06
N2903	4.13	2.44	0.06	1.25	0.06
N3198	3.87	3.16	0.06	0.53	0.01
N2403	2.22	2.64	0.11	1.34	0.06
N6503	3.82	2.19	0.05	1.09	0.03
N5585	0.39	0.46	0.07	2.02	0.20
N1560	1.30	0.71	0.07	1.01	0.03
N3109	0.25	0.25	0.05	2.51	0.14
D154	0.53	1.15	0.14	0.98	0.02

**Table A6.** NFW-CDMA-AC fits

Galaxy	$(M/L)_{\text{obs}}$ ( $M_{\odot}/L_{\odot}^R$ )	$(M/L)_{\text{epc}}$ ( $M_{\odot}/L_{\odot}^R$ )	Err.	$v_{\text{max}}^{\text{h,init}}$ ( $\text{km s}^{-1}$ )	Err. ( $\text{km s}^{-1}$ )	$R_s$ (kpc)	c	$F_{200}$
N2841b	3.52	0.80	0.10					
N2841d	2.06	0.71	0.12	250.5	3.0	24.63	11.03	0.051
N3992b	2.25	0.67	0.09					
N3992d	1.99	0.89	0.08	221.0	3.5	20.75	11.44	0.043
N7331b	2.54	0.55	0.02					
N7331d	1.20	0.57 (fix)		195.6	2.3	17.55	11.86	0.064
N2998	1.28	0.88	0.12	178.4	6.1	15.47	12.18	0.091
N2903	1.88	1.11	0.02	159.8	1.5	13.30	12.58	0.052
N3198	0.85	0.70	0.04	139.0	1.0	10.99	13.11	0.065
N2403	0.52	0.62	0.03	122.0	0.9	9.19	13.62	0.026
N6503	1.46	0.84	0.03	104.0	0.7	7.39	14.27	0.035
N5585	<0	<0		72.3	2.6	4.49	15.88	0.039
N1560	<0	<0		58.9	1.0	3.39	16.86	0.050
N3109	<0	<0		53.9	2.0	3.00	17.31	0.025
D154	<0	<0		39.2	0.9	1.94	19.00	0.066
N5585	0.85	1 (fix)		52.7		2.91	17.42	0.163
N1560	1.84	1 (fix)		54.0		3.01	17.30	0.092
N3109	1.01	1 (fix)		50.8		2.77	17.61	0.042
D154	0.46	1 (fix)		38.8		1.91	19.06	0.071

**Table A7.** Masses from observed stellar velocity dispersions for  $h/z_0 = 5$ 

Galaxy	Mass ( $10^9 M_{\odot}$ )	Err. ( $10^9 M_{\odot}$ )	$(M/L)_{\text{epc}}$ ( $M_{\odot}/L_{\odot}^R$ )	Err. ( $M_{\odot}/L_{\odot}^R$ )
N7331d	17.7	7.6	0.57	0.24
N3198	13.6	4.2	0.96	0.30
N6503	3.3	1.2	0.81	0.29
N2998	65.3 → 82.0	20%	1.19 → 1.49	0.27

**Table A8.**  $(M/L)_{\text{epc}} = 1.0$ , pseudo isothermal halo fits

Galaxy	Direct fit				Fit to a-de-contracted halo				$\rho_0^{\text{h}}$ ( $M_{\odot} \text{ pc}^{-3}$ )	Err. ( $M_{\odot} \text{ pc}^{-3}$ )
	$R_{\text{core}}$ (kpc)	Err. (kpc)	$v_{\text{max}}$ ( $\text{km s}^{-1}$ )	Err. ( $\text{km s}^{-1}$ )	$R_{\text{core}}$ (kpc)	Err. (kpc)	$v_{\text{max}}$ ( $\text{km s}^{-1}$ )	Err. ( $\text{km s}^{-1}$ )		
N2841	1.90	0.27	256.7	2.3	6.39	0.52	267.6	3.7	0.032	0.005
N3992	1.89	0.25	234.4	3.0	3.89	0.34	233.5	3.8	0.066	0.011
N7331	7.02	0.57	230.1	4.9	19.46	1.79	268.6	14.2	0.0035	0.0007
N2998	0.81	0.21	181.0	1.9	1.23	0.36	172.3	2.8	0.36	0.21
N2903	0.54	0.13	174.5	1.8	1.07	0.17	171.1	2.2	0.47	0.15
N3198	1.16	0.11	139.0	0.9	1.80	0.13	137.1	1.0	0.11	0.02
N2403	1.24	0.06	130.1	1.0	1.64	0.08	130.2	1.2	0.12	0.01
N6503	0.63	0.05	109.5	0.6	1.11	0.08	109.9	0.9	0.18	0.03
N5585	2.69	0.26	107.0	4.9	2.87	0.30	106.3	3.7	0.025	0.006
N1560	2.36	0.11	81.6	1.4	3.61	0.19	88.1	2.4	0.011	0.001
N3109	2.85	0.15	88.5	2.2	3.82	0.09	100.4	1.4	0.013	0.001
D154	1.18	0.05	51.8	2.7	1.44	0.08	53.2	3.4	0.025	0.002